



# On the efficient and sustainable utilisation of shallow geothermal energy by using borehole heat exchangers

Dissertation

zur Erlangung des akademischen Grades  
Doktoringenieur (Dr.-Ing.)

vorgelegt

der Fakultät Umweltwissenschaften  
der Technischen Universität Dresden

von

M.Sc. Philipp Sebastian Hein  
geb. am 16.04.1985 in Duisburg

Vorsitz:

Prof. Dr. Rudolf Liedl

Gutacher:

Prof. Dr. Olaf Kolditz

Prof. Dr. Peter Bayer

Prof. Dr. Stephan Schönfelder

Eingereicht im Dezember 2016

Tag der Verteidigung: 08.12.2017



---

## ÜBEREINSTIMMUNGSERKLÄRUNG

---

Die Übereinstimmung dieses Exemplars mit dem Original der Dissertation zum Thema:

*'On the efficient and sustainable utilisation of shallow geothermal energy by using borehole heat exchangers'*

wird hiermit bestätigt.

.....  
Ort, Datum

.....  
Unterschrift (Vorname Name)

---

## ABSTRACT

---

In the context of energy transition, geothermics play an important role for the heating and cooling supply of both residential and commercial buildings. Thereby, the increasingly and intensive utilisation of shallow geothermal resources bears the risk of over-exploitation and thus poses a future challenge to ensure the sustainability and safety of such systems. Particularly, the well-established technology of borehole heat exchanger-coupled ground source heat pumps is applied for the thermal exploitation of the shallow subsurface. Due to the complexity of the involved physical processes, numerical modelling proves to be a powerful tool to enhance process understanding as well as to aid the planning and design processes. Simulations can also support the management of thermal subsurface resources, planning and decision-making on city and regional scales. In this work, the so-called dual-continuum approach was adopted and enhanced to develop a coupled numerical model considering flow and heat transport processes in both the subsurface and borehole heat exchangers as well as the heat pumps' performance characteristics, and including the relevant phenomena influencing the underlying processes. Beside the temperature fields, the efficiency and thus the consumption of electrical energy by the heat pump is computed, allowing for the quantification of operational costs and equivalent carbon-dioxide emissions. The model is validated and applied to a number of numerical studies. First, a comprehensive sensitivity analysis on the efficiency and sustainability of such systems is performed. Second, a method for the quantification of technically extractable shallow geothermal energy is proposed. This procedure is demonstrated by means of a case study for the city of Cologne, Germany and its implications are discussed.

---

## ZUSAMMENFASSUNG

---

Im Rahmen der Energiewende nimmt die Geothermie eine besondere Rolle in der thermische Gebäudeversorgung ein. Die zunehmende, intensive Nutzung oberflächennaher geothermischer Ressourcen erhöht die Gefahr der übermäßigen thermischen Ausbeutung des Untergrundes und stellt damit eine wachsende Herausforderung für die Nachhaltigkeit und Sicherheit solcher Systeme dar. Zur Erschließung oberflächennaher geothermischer Energie wird insbesondere die etablierte Technologie Erdwärmesonden-gekoppelter Wärmepumpen eingesetzt. Aufgrund der daran beteiligten komplexen physikalischen Prozesse erweisen sich numerische Modelle als leistungsfähiges Werkzeug zur Erweiterung des Prozessverständnisses und Unterstützung des Planungs- und Auslegungsprozesses. Zudem können Simulationen zum Management thermischer Ressourcen im Untergrund sowie zur Planung und politischen Entscheidungsfindung auf städtischen und regionalen Maßstäben beitragen. Im Rahmen dieser Arbeit wurde, basierend auf dem sogenannten "dual-continuum approach" und unter Berücksichtigung des Einflusses der Wärmepumpe, ein erweitertes gekoppeltes numerisches Modell zur Abbildung der in Erdwärmesonden und dem Untergrund stattfindenden Strömungs- und Wärmetransportprozesse entwickelt. Das Modell ist in der Lage, alle relevanten Einflussfaktoren zu berücksichtigen. Neben den Temperaturfeldern im Untergrund und der Erdwärmesonde werden die Effizienz und damit der Stromverbrauch der Wärmepumpe simuliert. Damit können sowohl die Betriebskosten als auch der äquivalente CO<sub>2</sub>-Ausstoß abgeschätzt werden. Das Modell wurde validiert und in einer Reihe numerischer Studien eingesetzt. Zuerst wurde eine umfassende Sensitivitätsanalyse zur Effizienz und Nachhaltigkeit entsprechender Anlagen durchgeführt. Weiterhin wird ein Verfahren zur Quantifizierung des technisch nutzbaren, oberflächennahen geothermischen Potentials vorgestellt und anhand einer Fallstudie für die Stadt Köln demonstriert, gefolgt von einer Diskussion der Ergebnisse.

---

## ACKNOWLEDGEMENTS

---

First of all, I would like to thank my supervisor Olaf Kolditz (Faculty of Environmental Sciences, Dresden University of Technology and Department of Environmental Informatics, Helmholtz-Centre for Environmental Research Leipzig - UFZ). Also, I'd like to express my deepest gratitude to my supervisor and leader of the work group 'Geothermal Systems Analysis' Habing Shao (UFZ and Faculty of Geosciences, Freiberg University of Mining and Technology) for his continuous, patient and highly qualified guidance and support of my work, for countless fruitful discussions and constant encouragement. Furthermore, I'd like to thank Peter Bayer (TH Ingolstadt) and Stephan Schönfelder (HTWK Leipzig) for reviewing this thesis beside Olaf Kolditz. I want to acknowledge the funding of my work within in the project 'Entwicklung von Methoden zur standortoptimierten geotechnischen Auslegung großflächiger Geothermiesysteme - SAGS' under grant number 03FH059PX3 by the German Federal Ministry for Education and Research (BMBF). In this context, special thanks go out to the project leader Anke Bucher (Faculty of Mechanical and Energy Engineering, Leipzig University of Applied Sciences - HTWK) and project collaborator Uwe-Jens Görke (UFZ).

Many thanks to Anke Boockmeyer (Department of Geosciences, Kiel University) for the pleasant collaboration and discussions on BHE modelling, and to my office colleague Klodwig Seibertz (Department of Monitoring and Exploration Technologies, UFZ). Special thanks to Agnes Sachse for the collaboration on the tutorial book. I would also like to thank my ENVINF colleagues for their professional support on various topics like numerics, informatics and not to forget the lunch breaks to clear my mind from time to time. In this context, I'd especially like to mention Thomas Nagel, Tom Fischer, Marc Walther, Lars Bilke, Karsten Rink, Dmitri Naumov, Christoph Lehmann and Erik Nixdorf. I express my special appreciation to my old friend Nils Wolf for taking over the proofreading.

Last but not least, I'd like to thank my family. Without the continuous support of my parents I would never be where I am now. And of course and most importantly, my beloved ones, Klara and Onno.

*For Klara, Onno and Onkel Rudi.*

---

## CONTENTS

---

1	INTRODUCTION	1
1.1	Scope of this thesis	2
1.2	Outline of this thesis	2
<b>I</b>	<b>BACKGROUND, THEORY AND NUMERICS</b>	<b>3</b>
2	BACKGROUND	4
2.1	Geothermal energy	4
2.2	Borehole heat exchangers	5
2.3	Ground source heat pumps	9
2.4	Influencing factors	12
2.5	Literature review	13
3	THEORY	16
3.1	Heat transfer	16
3.2	Groundwater flow	19
4	NUMERICS	21
4.1	Dual-continuum approach	21
4.2	Finite element realisation	24
4.3	Heat pump model	27
5	MODEL VALIDATION	28
5.1	Experimental setup	28
5.2	Model setup	29
5.3	Results	29
<b>II</b>	<b>APPLICATIONS</b>	<b>32</b>
6	SUSTAINABILITY AND EFFICIENCY OF BHE-COUPLED GSHP SYSTEMS	34
7	QUANTIFICATION OF TECHNICALLY EXPLOITABLE SHALLOW GEOTHERMAL ENERGY	36
8	TECHNICALLY EXPLOITABLE SHALLOW GEOTHERMAL ENERGY: CASE STUDY	38
<b>III</b>	<b>SUMMARY</b>	<b>40</b>
9	ACHIEVEMENTS	41
10	CONCLUSIONS AND OUTLOOK	43
	APPENDIX	53
1	Paper 1	53
2	Paper 2	53
3	Paper 3	53



---

## NOMENCLATURE

---

### Greek symbols

$(\rho c)$	Volumetric heat capacity	$[\text{Jm}^{-3}\text{K}^{-1}]$
$\alpha$	Heat transfer coefficient	$[\text{Wm}^{-2}\text{K}^{-1}]$
$\Delta T_{s,eq}$	Equivalent temperature drop	$[\text{°C}], [\text{K}]$
$\Delta$	Difference operator	
$\delta$	Optimal nodal distance	$[\text{m}]$
$\epsilon$	Porosity	$[-]$
$\Gamma$	Boundary	
$\lambda$	Thermal conductivity	$[\text{Wm}^{-1}\text{K}^{-1}]$
$\nabla$	Nabla operator	
$\Omega$	Integration domain	
$\omega$	Test function, trial function	
$\Phi$	Heat transfer coefficient	$[\text{Wm}^{-2}\text{K}^{-1}]$
$\rho$	Density	$[\text{kgm}^{-3}]$
$\theta$	Saturation	$[-]$
$r_b$	Borehole radius	$[\text{m}]$

### Indices

$0$	initial state
<b>B</b>	BHE
<b>S</b>	Soil, subsurface
$e$	Finite element
$eff$	effective
$f$	fluid
$g$	Grout
$geo$	geothermal
$i$	Inlet pipe

$k$	BHE components
$n$	Previous time step/iteration
$n + 1$	Current time step/iteration
$o$	Outlet pipe
$s$	soil, subsurface

### Roman symbols

$\Delta t_n$	Time step size	[s]
$\dot{Q}$	Heat flux	[W]
$\dot{W}$	Power density	[Wm <sup>-3</sup> ]
<b>H</b>	Column matrix of source terms	
<b>L</b>	Laplace matrix	
<b>M</b>	Mass matrix	
<b>n</b>	Normal vector	
$\mathbf{q}_D$	Darcy flux	[ms <sup>-1</sup> ]
$\mathbf{q}_n$	Heat flux in normal direction	
$\mathbf{q}$	Vector of heat flux density	[Wm <sup>-2</sup> ]
<b>R</b>	Heat exchange matrix	
<b>T</b>	Column matrix of temperatures	
$\mathbf{v}$	Velocity vector of heat carrier fluid	[ms <sup>-1</sup> ]
$A$	Area	[m <sup>2</sup> ]
$c$	Specific heat capacity	[Jkg <sup>-1</sup> K <sup>-1</sup> ]
$CO_{2e}$	Carbon-dioxide equivalent	[°C], [kg]
$COP$	Coefficient of performance	[-]
$E$	Energy	[J]
$G$	Source term (groundwater flow equation)	[ms <sup>-1</sup> ]
$h$	Hydraulic head	[m]
$k_f$	Hydraulic conductivity	[ms <sup>-1</sup> ]
$N$	Trial function space	
$P$	Power	[W]

$Q$	Thermal energy, heat	[J]
$q$	Heat flux density	[Wm <sup>-2</sup> ]
$Q_h$	Volumetric flow rate of heat carrier fluid	[m <sup>3</sup> s <sup>-1</sup> ]
$q_{geo}$	Geothermal heat flux density	[Wm <sup>-2</sup> ]
$R$	Thermal resistance	[mKW <sup>-1</sup> ]
$S$	Specific heat exchange surface	[m]
$S_s$	Storage coefficient (groundwater flow equation)	[-]
$SCOP$	Seasonal coefficient of performance	[-]
$T$	Temperature	[°C], [K]
$t$	Time	[s]
$U$	Internal energy	[J]
$u$	Specific internal energy	[Jm <sup>-3</sup> ]
$V$	Volume	[m <sup>3</sup> ]
$v_D$	Darcy velocity	[ms <sup>-1</sup> ]
$W$	Work	[J]

---

## ACRONYMS

---

<b>BC</b>	Boundary condition
<b>BHE</b>	Borehole heat exchanger
<b>BTES</b>	Borehole thermal energy store
<b>COP</b>	Coefficient of performance
<b>DCA</b>	Dual-continuum approach
<b>DOF</b>	Degree of freedom
<b>FLS</b>	Finite line source
<b>GFEM</b>	Galerkin Finite Element Method
<b>GSHP</b>	Ground source heat pump
<b>HVAC</b>	Heating, ventilation and air conditioning
<b>IC</b>	Initial condition
<b>ILS</b>	Infinite line source
<b>MILS</b>	Moving infinite line source
<b>MFLS</b>	Moving finite line source
<b>OGS</b>	OpenGeoSys
<b>PE</b>	Polyethylene
<b>SCOP</b>	Seasonal coefficient of performance
<b>TCRM</b>	Thermal capacity-resistor model
<b>THMC</b>	Thermo-hydro-mechanical-chemical

---

## INTRODUCTION

---

In recent years, the shallow subsurface is increasingly utilised as a renewable and decentralised source of thermal energy for the heating and cooling of both residential and commercial buildings. Most commonly, borehole heat exchanger (BHE)-coupled ground source heat pump (GSHP) systems are deployed for this purpose. In some cases, BHEs are installed with a high area-specific density, either resulting from big building projects with a single system containing a large number of BHEs, or various individual systems in a newly developed residential area. Such scenarios can lead to an intensified thermal exploitation of the underground. Thus, the management of the shallow subsurface, aiming at a sustainable utilisation, poses a future challenge [1].

In practice, a number of problems occur frequently [2]. For example, under-dimensioning, construction errors and interaction between BHEs or neighbouring GSHP systems are likely to result in over-exploitation of the subsurface. A possible consequence is ice formation, leading to damage of building foundations, BHE pipes and grouting. More often, the efficiency of the GSHP is decreased, causing increased electricity costs and thus an uneconomical operation of the system. In the worst case, the heat carrier fluid temperature drops below a certain level, so that it triggers a protective shut-down of the heat pump [3]. On the other side, over-dimensioning of the GSHP system leads to increased investment costs, which becomes more remarkable in projects where a large number of BHEs is installed.

The heat transfer processes related to the operation of BHE-coupled GSHP systems are rather complex and influenced by a large number of factors, including the local subsurface properties, groundwater flow, thermal regime of both the soil and the ground surface, system design and loading scenarios. Although the technology is already established for several decades, the process understanding still needs to be enhanced, specifically with respect to challenges evoking from the increasingly intensified utilisation of shallow geothermal resources, as well as efficiency and safety issues. Scientific insights should be integrated into existing design concepts, which need to be further developed in order to increase the efficiency and cost effectiveness of such systems and reduce potential risks. This also holds true for

approval activities to ensure sustainability of the thermal subsurface regime.

### 1.1 SCOPE OF THIS THESIS

As in real world scenarios the heat transport and flow processes inside BHEs and the surrounding subsurface are quite complex, numerical models prove to be a powerful tool for the simulation of such systems. A numerical BHE model, based on the so-called dual-continuum approach was implemented in OpenGeoSys (OGS), an open-source Finite Element-code for the simulation of coupled thermo-hydro-mechanical-chemical (THMC) processes. In this work, the original implementation of the BHE model is enhanced, amongst others with a coupled heat pump model, to allow for realistic and accurate simulations of BHE-coupled GSHP systems. With this extension, the heat pump's dynamic electricity consumption can be quantified, which allows for financial analyses and the estimation of equivalent CO<sub>2</sub> emissions. The numerical model is applied to investigate the behaviour of such systems under various conditions and thus to enhance process understanding. More precisely, the most important parameters influencing the efficiency of GSHPs are identified and quantified. As a tool for planning, thermal subsurface management and policy making, a method for the quantification of sustainably and efficiently exploitable shallow geothermal energy is developed. The proposed work flow is demonstrated with a case study.

### 1.2 OUTLINE OF THIS THESIS

This thesis consists of three parts. In the first one, the technical background of BHE-coupled GSHP systems and a summary of the relevant literature is provided, together with the theory of heat transport and groundwater flow. The numerical model employed in this work is presented and validated. The model was applied to carry out several investigations. In the second part, the numerical investigations are presented as a series of two peer-reviewed and published research papers, as well as one submitted paper. In the last part, this work is summarised and the results are concluded. Also, an outlook to further research topics is given in the end.

Part I

BACKGROUND, THEORY AND NUMERICS

---

## BACKGROUND

---

In this chapter, an overview of geothermal energy and its utilisation as well as the technical background and working principles of BHEs and GSHP systems are given. The factors that influence the heat transport and flow processes of such systems are summarised, and the relevant literature in this field is reviewed.

### 2.1 GEOTHERMAL ENERGY

In recent years, the utilisation of renewable energies is steadily increasing. Regarding the production of thermal energy, biomass is the leading energy source, followed by solar heat and geothermal energy [4]. The importance of geothermal energy is supposed to increase on a long-term perspective, as

- it is a renewable energy source.
- it can be utilised almost anywhere on earth.
- it is inexhaustible, when utilised in a sustainable manner.
- it is able to supply basic load.
- it is environmental friendly.
- it requires little space on the surface.

The thermal regime of the subsurface is controlled by a number of factors, with a complex heat flux field variable both spatially and temporally [4]. The temperature at the earth's core is about 5000 °C, while the mean surface temperature is approximately 14 °C. By this temperature difference, a steady heat flux directed towards the earth's surface is induced, with a mean magnitude of 0.065 Wm<sup>-2</sup>. In the earth's crust, the mean geothermal gradient is about 0.03 °Cm<sup>-1</sup>. In other words, the temperature increases by 3 °C per 100 m depth. At the same time, solar energy hits the earth's surface. Approximately 30 % of the solar radiation is reflected, while approximately 20 % are absorbed by the atmosphere and the other 50 % are absorbed by the ground. As the largest part of these 50 % are again emitted to the atmosphere through radiation and convection, only a small portion finally contributes to the warming of the ground surface. With respect



to daily cycles, the ground surface temperature fluctuations propagate a couple of decimeters into the subsurface. In an annual cycle, the propagation depth is approximately 10-20 m. It should be noticed though, that the heat fluxes from and to the ground surface are highly dependent on local conditions, e.g. thermal anomalies of the subsurface (e.g. convection in fault zones) and different land cover like buildings, asphalt, soil, vegetation etc. (cf. [5]) and the spatial scale under consideration (meso-, local-, or microscale). Furthermore, in urban areas the shallow subsurface is exposed to anthropogenic heat fluxes, e.g. arising from sewage water systems, underground railways etc., contributing to the so-called urban heat island effect (cf. [6]).

For the application of geothermal energy, it is usually differentiated between shallow and deep geothermics (sometimes a medium depth is considered as well). The boundary is drawn at a depth of 400 m. Another classification is based on the reservoir temperature, which leads to either low- or high-enthalpy systems. The boundary here is often drawn at approximately 200 °C. As a result, the shallow subsurface is by nature a low-enthalpy reservoir. While high enthalpy reservoirs are usually exploited by steam turbines for power generation, low enthalpy geothermal energy is mostly applied for heating purposes. Here the temperature level has to be lifted, which is commonly achieved by a heat pump.

Regarding shallow geothermal systems, it is differentiated between open- and closed-loop systems. In open-loop systems, groundwater is pumped from the aquifer and re-injected after the heat has been extracted by the heat pump. This is typically realised with two wells. In closed-loop systems, a heat carrier fluid (mostly water with anti-freezer) is circulated through heat exchanger pipes. Horizontal ground heat exchangers are buried at a depth of 1-2 m below the land surface, with the pipes arranged as coils. To extract the desired amount of heat, the pipes are several hundred meters long, which requires a high demand of available free surface area. Strictly speaking, due to their limited depth, horizontal ground heat exchangers utilise solar heat rather than geothermal energy.

## 2.2 BOREHOLE HEAT EXCHANGERS

BHEs are mostly installed in vertical cylindrical boreholes with a depth of several tens of meters up to several hundred meters, although inclined boreholes are sometimes also installed. The actual heat exchanger is realised whether as single (1U) or double (2U) U-shaped pipes or with an coaxial pipe-in-pipe arrangement (cf. Fig. 1). Coaxial BHEs are further differentiated into CXC and CXA types. In the former one, the inlet pipe is centered in the outlet pipe. In the latter, the configuration of inlet and outlet is swapped. The space

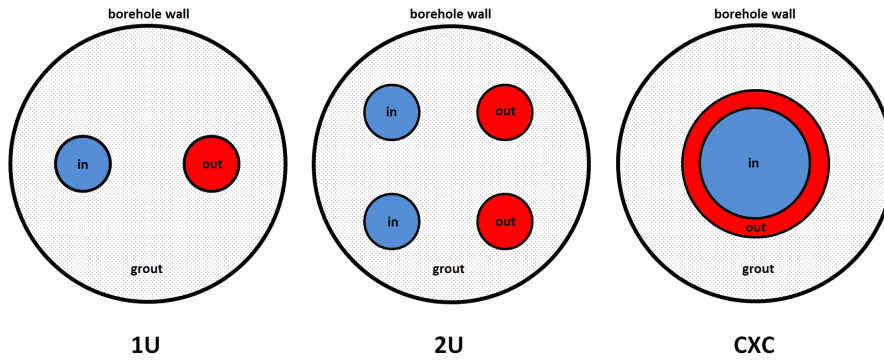


Figure 1: Schematic illustration of different BHE types in the heating mode. When applied for cooling applications, either the flow direction or the functionality of inlet and outlet pipes are reversed.

between the pipes and the borehole wall is usually filled with a grouting material like bentonite or cement. In Scandinavian countries, it is common to fill the void space with water.

When the GSHP system is applied for heating, the heat carrier fluid is circulated through the pipes. The pumping rate is usually chosen such that a turbulent flow is established. This is beneficial, as the convective heat transfer between the fluid and the pipe walls is substantially higher than in the case of laminar flow. The fluid, which is colder than the surrounding soil or rock, is transported through the pipe. Due to the temperature difference between the fluid, grout and surrounding soil, a heat flux, directed from the soil to the inner of the BHE, is induced. The fluid adsorbs heat from the underground and is heated up, as illustrated for a 1U BHE in Fig. 2. The fluid is then pumped from the outlet pipe to the heat exchanger in the evaporator stage of the heat pump, where the extracted energy is utilised. By this, the fluid is cooled down again and re-enters the BHE at the inlet pipe. For cooling and heat storage applications, the process runs in reverse. In other words, a warm fluid is circulated through the BHE and releases energy to the subsurface.

Another BHE concept works with the phase change of a refrigerant fluid acting as the heat carrier. In most cases, this is carbon dioxide. Under high pressure, cold and liquid  $\text{CO}_2$  flows downwards at the inner pipe wall, extracts heat from the vicinity and thus evaporates. The gaseous  $\text{CO}_2$  then rises to the top of the BHE, where it undergoes another phase change in the heat pump and re-enters the BHE again in its liquid state. This type of BHE is not the subject of this work.

The borehole diameter usually ranges from 120-150 mm. The pipes are mostly manufactured from polyethylene (PE) with a relative low thermal conductivity of  $0.4 \text{ Wm}^{-1}\text{K}^{-1}$ . Typical diameters for U-shaped pipes are 32 mm with a wall thickness of 2.9 mm. Together with the

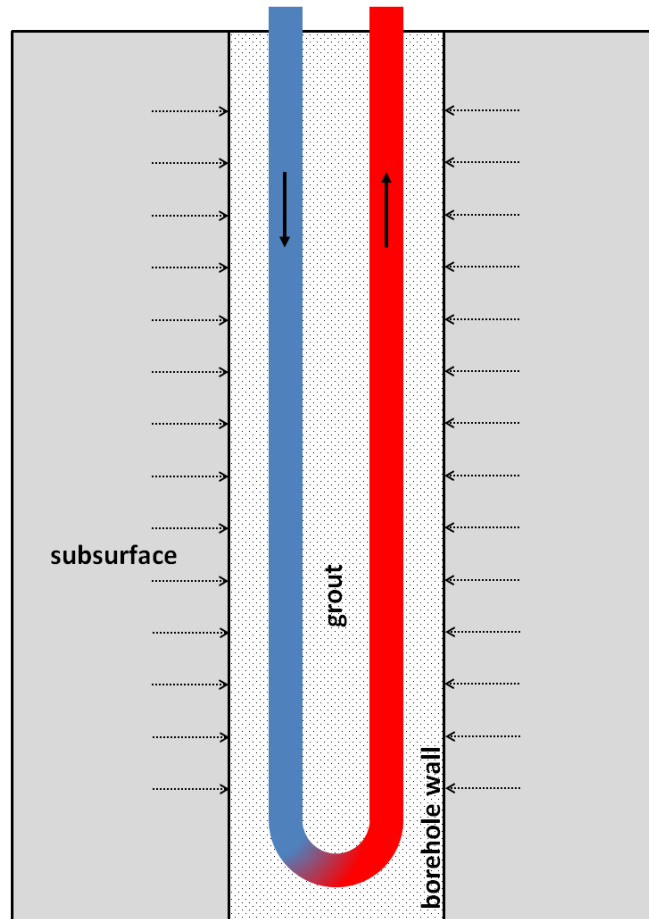


Figure 2: Schematic illustration of a 1U BHE in heating mode. The bold vertical arrows indicate the flow direction. Heat flux is indicated by dotted horizontal arrows. When applied for cooling applications, either the flow direction or the functionality of inlet and outlet pipes are reversed. The direction of heat flux is then reversed as well.

pipes, spacers should be installed to avoid any contact between them, which may lead to a thermal short-circuit. For the grouting, bentonite with a thermal conductivity of approximately  $0.8 \text{ Wm}^{-1}\text{K}^{-1}$  is widely used, although thermally enhanced grouting materials with thermal conductivities in the range of  $2.0 \text{ Wm}^{-1}\text{K}^{-1}$  are already available. Beside ensuring the connection between the pipes and the borehole wall, respectively the surrounding subsurface, the grout acts as a sealing. This is to prevent hydraulic short-circuits, in case that the borehole penetrates different aquifers. Another requirement regarding the grout is frost resistance. In general, for all involved materials a high thermal conductivity is desired. For the heat carrier fluid, a high thermal conductivity and volumetric heat capacity is beneficial for the thermal process. With respect to hydraulic properties, a low

dynamic viscosity and density is favourable to reduce the pumping capacity of the circulation pump for economical reasons. Virtually all components of BHEs are subject to ongoing research and development in order to improve their thermal and hydraulic properties as well as safety aspects. Finally, one or more BHEs are coupled to a heat pump. For the system integration, which is not subject of this work, additional piping and components like distributors, collectors, mountings and pumps are required.

BHEs are most commonly applied for heating together with a heat pump. In this case, the subsurface in the vicinity of the BHE(s) is cooled down. With pure heat conduction, the resulting temperature field is funnel-shaped (e.g. see Fig. 4 in App. 2). In summer, when the heat pump is switched off, the subsurface temperature partially recovers. Thus, two effects occur: First, the fluid and subsurface temperatures fluctuate annually, due to a varying heat pump load (e.g. see Fig. 1 in App. 2), respectively the buildings heat demand, and the recovery process in summer, when the heat pump is switched off. Second, a long-term decay process takes place. This is due to the fact, that the thermal load on the subsurface is unbalanced. For example, both effects are observable (cf. Fig. 5 in App. 2) in the subsurface temperature evolution at the BHE wall. A recovery of the temperature field is only achieved by heat fluxes from the top (ground surface temperature) and bottom (geothermal heat flux), as well as lateral fluxes due to a horizontal temperature gradient. This can be interpreted such that heat from undisturbed regions flows into the temperature funnel induced by the BHE. As a consequence, a dynamic equilibrium or quasi-steady state will be achieved over the course of 10-15 years. When noticeable groundwater flow is present, it will facilitate the recovery, as additional energy is transported into the system. In this case, the quasi-steady state usually will be reached earlier.

BHEs can also be utilised for additional cooling in summer, with different eligible technologies. Some heat pumps can be run in reverse, such acting as a cooling unit. The waste heat arising from this process is then injected into the subsurface through the BHE. When other active cooling technologies like conventional air-conditioning are applied, the heat pump is bypassed, while the excess heat is again transported to the subsurface via BHEs. This principle also applies for direct cooling techniques like concrete core cooling. BHEs can further be utilised for heat storage. For example, solar heat which is obtained in summer can be stored in the subsurface. The combined application for heating and cooling is in general beneficial, as the storage or injection of heat during the summer months facilitates the subsurface temperature recovery, leading to a more balanced thermal load. Detailed analyses on the impact of BHE operation on the subsurface temperature field are carried out in the main part of this thesis in Chapters 6-8.

The most important design parameters of BHEs are the subsurface thermal conductivity, heat pump or BHE load and the annual hours of operation. In Germany, the dimensioning is regulated by the VDI 4640 guideline [7], [8]. However, the BHE design is closely connected to the entire building services, which can be quite complex including different heat and cold sources and users, buffer tanks, control systems, heat pump operation modes, etc. For example, the number of annual hours of operation strongly depends on whether the BHE system is supposed to be the exclusive heat supply or if it is combined with other heat sources like solar heat, conventional gas heating etc. Thus, a correctly designed BHE field doesn't guarantee the proper operation of the system, as the integration of different HVAC components and their control is a crucial factor.

### 2.3 GROUND SOURCE HEAT PUMPS

Heat pumps rely on a power and heat process. With the aid of mechanical work, thermal energy is extracted from a low temperature reservoir (here the BHE circuit), respectively the heat source, and lifted to a higher temperature level suitable for the desired utilisation (here space heat and hot water supply), respectively the heat sink. By this, thermal energy is moved in the opposite direction of spontaneous heat flow. The reverse process is applied in cooling units like air-conditioners and refrigerators, absorbing thermal energy on a high temperature level which is partially converted in mechanical work and releasing the remaining energy as waste heat on a low temperature level.

The most common type of heat pumps is based on a vapor-compression refrigerant cycle (cf. Fig. 3). Here, the refrigerant is circulated in a closed loop. The cold and gaseous working fluid under low pressure enters the compressor stage (1). It leaves the compressor on the discharge side as hot vapour under high pressure. In the condenser stage it now enters a heat exchanger (2), where it condenses to a high pressure liquid with moderate temperature. In the heat exchanger at this stage, high temperature thermal energy is released to the buildings heating circuit, acting as the heat sink. In the next stage, the liquid enters an expansion valve (3), where the pressure and temperature are further reduced. Finally, the liquid enters the evaporator stage (4) with another heat exchanger. The refrigerant absorbs low temperature heat from the BHE, which acts as the heat source. The fluid starts to boil and thus evaporates, and then leaves the evaporator as a cold, low pressure gas before re-entering the compressor (1). In the heat exchanger at the evaporator stage (4), the warm fluid in the BHE circuit releases its heat to the heat pump refrigerant. In other words, at this point the geothermal energy is utilised. The cold fluid in the buildings heating circuit enters the heat exchanger of the

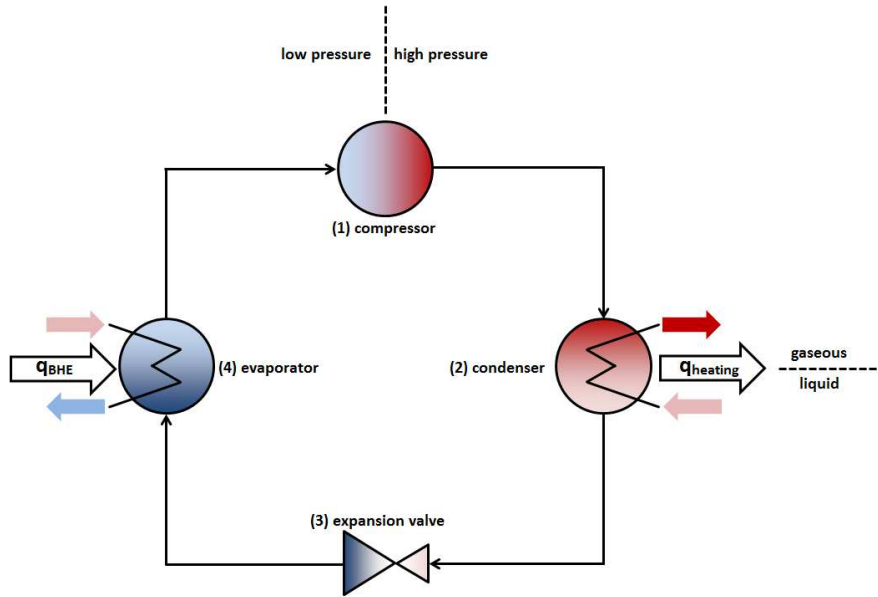


Figure 3: Schematic working principle of a heat pump. The refrigerant temperature level is color coded, with increasing temperature from light blue to dark red.

condenser stage (2), where it absorbs the thermal energy on a now lifted temperature level.

The compressor is in most cases driven by an electric motor, while some types also operate with oil or gas engines. For the refrigerants, hydro-fluorocarbon, ammonia, propane, butane and carbon dioxide are used, which have different advantages and drawbacks regarding efficiency, inflammability and environmental friendliness such as impact on ozone layer and greenhouse effect. It should be mentioned that some heat pumps are capable of running in reverse, so that both heating and cooling can be provided. Beside compression heat pumps, which are exclusively considered in this work, other concepts are existing. These are absorption and adsorption heat pumps. The former ones make use of reaction heat arising from the mixture of two liquids or gases. The latter ones are based on solid solvents, on which the refrigerant is cyclically adsorbed and desorbed and thus releasing and taking up the heat.

The efficiency of heat pumps is usually measured in terms of *coefficient of performance* (COP), which is the ratio of useful heat  $Q$  supplied by the heat pump and the work  $W$  carried out by the heat pump to supply this amount of heat.

$$COP = \frac{Q}{W}. \quad (1)$$

More specifically, as heat is supplied to or removed from a building, we write  $Q_{Building}$  instead of  $Q$ . In heating mode, a certain amount of thermal energy  $Q_{BHE}$  is extracted from the subsurface (the reservoir)

with BHEs. With additional electrical energy  $W$ , consumed by the compressor, the temperature level is elevated, such that

$$Q_{Building}^{heating} = Q_{BHE}^{heating} + W \quad (2)$$

and consequently

$$COP^{heating} = \frac{Q_{Building}^{heating}}{W} = \frac{Q_{BHE}^{heating} + W}{W}. \quad (3)$$

It should be noticed that in the above equations, the heat loss along connecting pipelines is not considered. In case of cooling, a certain amount of heat  $Q_{Building}^{cooling}$  is removed from the building while investing a certain amount of electrical energy  $W$ . Now, on the discharge side of the heat pump, both the removed heat and the heat arising from compression (the converted electrical energy) are transported to the BHE, such that

$$Q_{BHE}^{cooling} = Q_{Building}^{cooling} + W. \quad (4)$$

Thus, the COP for cooling reads

$$COP^{cooling} = \frac{Q_{Building}^{cooling}}{W}. \quad (5)$$

For example, in heating mode and operating with a  $COP^{heating}$  value of 4, the heat pump supplies 4 kWh of heat while investing 1 kWh of electrical energy. The heat extracted from the subsurface is then 3 kWh. In cooling mode, operating with a  $COP^{cooling}$  of 3, 3 kWh of heat are removed from the building while investing 1 kWh of electrical energy. The corresponding amount of thermal energy injected into the subsurface is 4 kWh.

To analyse how the COP is affected by source and sink temperatures in heating mode, we replace  $Q_{building} = Q_{sink}$  and  $Q_{BHE} = Q_{source}$ . Substituting these definitions into Eq. (2) and solving for  $W$  yields  $W = Q_{sink} - Q_{source}$ . Now, substituting this into Eq. (3) yields

$$COP^{heating} = \frac{Q_{sink}}{Q_{sink} - Q_{source}}. \quad (6)$$

By making use of *Carnot's theorem* [9], it can be shown that

$$COP^{heating} = \frac{T_{sink}}{T_{sink} - T_{source}}, \quad (7)$$

with absolute temperatures  $T_{sink}$  and  $T_{source}$ . Applying the same procedure for cooling mode yields

$$COP^{cooling} = \frac{Q_{source}}{Q_{sink} - Q_{source}} = \frac{T_{source}}{T_{sink} - T_{source}}. \quad (8)$$

Sink and source sides of the heat pump are now swapped, as the buildings circuit is the source and the BHE acts as the sink. As can

be clearly seen, the COP and such the efficiency increases with decreasing temperature difference  $T_{sink} - T_{source}$  in both cases. Usually, the temperature in the building circuit is more or less fixed. For example, radiators require a temperature of 50 °C or more, while floor heatings typically operate with a temperature of 35 °C. Thus it is beneficial to design the heating and cooling facilities such that the required temperatures are as low as possible. As a consequence, once a system installed, the main influencing factor on the COP is the BHE outlet temperature, such that  $COP = f(T_{out})$ . By this, COP is a momentary quantity, which depends on the heat pumps performance characteristics, its load and the BHE outlet temperature. Characteristic COP curves are usually provided with data sheets from the heat pump manufacturers. As a realistic indicator of the energy efficiency throughout a whole year, the *seasonal COP* (SCOP) is employed by accounting the total  $Q$  and  $W$  supplied and consumed in this period

$$SCOP = \frac{\int_{t_0}^{t_1} Q dt}{\int_{t_0}^{t_1} W dt}. \quad (9)$$

#### 2.4 INFLUENCING FACTORS

In the preceding sections, a number of parameters which influence the operation of BHE-coupled GSHP systems were already mentioned. To provide a brief overview, these are subsequently summarised.

The thermal properties, specifically the thermal conductivity  $\lambda$  and the volumetric heat capacity ( $\rho c$ ) with density  $\rho$ , are the main parameters for heat transfer. In general, the higher these values are, the better is the ability of a certain material to transport and store heat. Thus, the thermal properties of all involved materials like subsurface, BHE components as well as groundwater and heat carrier fluid, considerably influence the overall characteristics of the heat transport processes. As the subsurface consists of porous media, the porosity  $\epsilon$  and saturation  $\theta$  affect the effective thermal properties as well. Also, the subsurface is layered, meaning it consists of different stratigraphic units with different properties.

When noticeable groundwater flow is present, the subsurface temperature field is also subject to heat advection. For example, BHE-coupled GSHP systems usually perform more efficiently with increased groundwater flow velocity, due to an elevated temperature level in the vicinity of the BHE (cf. Chaps. 6 & 7), while in case of heating a cold plume is produced and transported in flow direction, possibly affecting other GSHP systems located downstream. The most important parameter here is the Darcy velocity  $v_D$ .

Furthermore, the local thermal regime of a specific site is of interest. It is determined by the local geothermal gradient  $(\frac{\partial T}{\partial z})_{geo}$ , geothermal



heat flux density  $q_{geo}$  and the temporally fluctuation of the ground surface temperature  $T_{gs}(t)$ . In general, the higher the subsurface temperature is, the higher the BHE fluid temperatures and thus the heat pump efficiency will be.

Of course, the system design including BHE types, material and geometry as well as the number, arrangement and interconnection of the BHEs, greatly affect the overall behavior. This further includes different operational modes (heating only, additional cooling, etc.), operational parameters like flow rate and the heat pump load as well as its performance characteristics.

With BHE fields, complex interactions between the individual BHEs strongly influence the resulting temperature field in the underground. This also holds true, when in practice other GSHP systems are installed in the neighbourhood, possibly leading to competing utilisation of shallow geothermal energy.

## 2.5 LITERATURE REVIEW

In the following section, a concise overview of the relevant scientific works regarding BHE-coupled GSHP systems is presented. In the research papers constituting Part II of this work, the outcome of these works is summarised and analysed more detailed, and set into the context of the influencing factors presented in the preceding section, to point out some research gaps which partially should be closed through the work presented in this thesis.

A common approach to analyse the subsurface temperature field in response to BHE operation is to employ analytical solutions. Stauffer et al. [10] provide a comprehensive collection of different kinds of analytical models. Namely, the most important one is the *infinite line source* (ILS) model, from which other models are derived. For example, to account for vertical effects, the *finite line source* (FLS) model is employed. To consider advection through groundwater flow, both of the aforementioned solutions can be enhanced to *moving ILS* (MILS) and *moving FLS* (MFLS) models (cf. Molina-Giraldo et al. [11]). In models simulating both the subsurface and BHE fluid temperatures, line-source or other models for the response of the subsurface are employed as so-called g-functions together with the thermal borehole resistance, which is usually also based on models. The first realisation of this approach, suitable for practical applications, was developed by Eskilson [12]. Also, a model for the heat transport processes inside the BHE was introduced in Eskilson's work, which is based on a thermal network analog to electrical circuits. A recent analysis of different models based on g-functions was presented by Li and Lai [13]. Further analytical models, based on Laplace transforms of the heat equation, were proposed by Beier [14] as well as Claesson and Javed [15]. All analytical models are derived by means of simplifying

assumptions, such that they are not capable of simulating complex systems including all relevant factors of influence.

Amongst others, Angelotti et al. [16] investigated the impact of groundwater flow velocity on the performance of BHEs by means of a numerical model. Luo et al. [17] investigated the performance of a BHE in a layered subsurface, including an aquifer. The numerical results showed that the BHE length can be reduced in comparison to a homogeneous subsurface model, while achieving the same efficiency. Perego et al. [18] performed numerical simulations of a medium scale BHE array in a layered subsurface. They concluded that employing a homogeneous subsurface assumption, the thermal impact on the underground is strongly underestimated.

Both Rivera et al. [5] and Bandos et al. [19] presented analytical solutions which are able to consider the thermal regime of a site, specifically the geothermal gradient and ground surface fluctuation. Kurevija et al. [20] investigated the effect of ground surface temperature and geothermal gradient on the dimensioning of BHEs, concluding that neglecting both quantities leads to an over-dimensioned BHE length. Bidarmaghz et al. [21] performed a similar analysis on the influence of the surface temperature fluctuation. They come to similar conclusions, that when the surface temperature fluctuation is considered in the design process, the BHE length can be reduced up to 11%. Regarding the numerical modelling approach, Bortoloni et al. [22] analysed the impact of different boundary conditions at the top surface. They conclude that imposing a Dirichlet boundary condition, i.e. the temporally variable ground surface temperature, yields accurate results.

De Paly et al. [23] and Beck et al. [24] proposed analytical solutions for BHE arrays. In the first work, a method for the optimisation of loading of the individual BHEs is presented. In the latter work, the geometric arrangement of the BHE array is optimised additionally. A similar study was conducted by Yu et al. [25], who developed a zoning strategy, in which different BHEs operate at different times to minimise the thermal impact on the subsurface. Retkowksi et al. [26] evaluated optimised heat extraction strategies for BHE arrays by means of a FLS model. Also based on an analytical approach, Koohi-Fayegh and Rosen [27] developed a model to examine the influence of thermal interaction between multiple BHEs on the heat pump efficiency. Kurevija et al. [28] compared different geometrical BHE arrangements and their implication for the actual dimensioning of required loop length by means of numerical simulations. The effect of BHE spacing in an array on the thermal performance was investigated by Gultekin et al. [29]. They found that in the investigated system, with a spacing of 4.5 m the performance loss is less than 10%.

Suitable models for the simulation of transient heat transport processes due to short-term operational cycles were proposed by De Rosa et al. [30] and Dai et al. [31]. Erol et al. [32] investigated the sustainability and recovery of the subsurface temperature distribution in response to BHE operation with an analytical model. Addressing the same topic, Sliwa and Rosen [33] presented a review of natural and artificial processes which facilitate the thermal regeneration of the underground. Mielke et al. [34] investigated the impact of a borehole thermal energy store (BTES) on the subsurface.

In all of the above mentioned studies, only single or a few aspects relevant to the sustainability and efficiency of BHE systems are investigated.

Desmedt et al. [35] conducted an experimental analysis of the performance of different BHE types and grouting materials. Similar investigations were carried out by Wood et al. [36] and Lee et al. [37]. Casasso et al. [38] performed a comprehensive numerical sensitivity analysis, investigating the effect of various parameters on the efficiency of GSHP systems.

From a practical perspective, Hähnlein et al. [1] compared the legal status of shallow geothermics in different countries. They concluded that comprehensive 3D planning and management methods are required to ensure a sustainable utilisation of shallow thermal resources. Epting et al. [39] come to similar conclusion. Blum et al. [40] assessed technical and economical factors influencing the design and performance of BHE-coupled GSHP systems in Germany. They found, that subsurface properties are not adequately considered during planning and design of such systems, causing under- and overdimensioned systems and such impacting the economic efficiency.

Zhu et al. [6] estimated the geothermal potential of Cologne, Germany. This paper serves as a foundation for the work presented in Chapters 7 & 8. Further studies regarding the shallow geothermal potential were performed by Arola and Korkka-Niemi [41] and Arola et al. [42] for sites in Finland and by Zhang et al. [43] for the City of Westminster, London, UK.

---

## THEORY

---

In this chapter, the mathematical framework of heat transfer and groundwater flow is provided along with the corresponding governing equations, as these are the processes involved in the operation of BHE-coupled GSHP systems. For simplicity, the following assumptions are made:

- Constant material properties. In general, density, viscosity, heat capacity and thermal conductivity are temperature-dependent. However, for the temperature ranges relevant for the processes considered in this work, it is safe to assume constant, temperature-independent properties.
- Isotropic thermal and hydraulic conductivity.
- Fully saturated porous media.
- Heat dispersion is neglected.

However, the actual OGS implementation is capable of dealing with variable material properties, anisotropic conductivities and heat dispersion in partially saturated media.

### 3.1 HEAT TRANSFER

Heat transfer is the transport of thermal energy, which is also considered as heat, in or between physical systems, resulting in a change of internal energy. The physical quantity of heat transfer is the heat flux, which is driven by a temperature gradient. Specifically, heat flows always in the direction of lower temperatures. Beside the temperature field, the thermal material properties determine the heat transfer process. These are the thermal conductivity, which reflects the ability to conduct heat in a material as well as the heat capacity, which reflects the ratio of transferred heat and the resulting temperature change. It can be interpreted as the ability of a material to store heat due to a temperature change. Heat can be transferred by four mechanisms:

- Conduction or diffusion: Energy is transferred inside a medium due to the exchange of kinetic energy between atoms or molecules without mass transport. Thus, conduction also takes place when

two or more systems are in physical contact without mass transport.

- Radiation: Heat is transferred through electromagnetic radiation.
- Advection: Heat is *transported* in a moving fluid. Strictly speaking, energy is moved due to mass transport and thus doesn't represent a heat *transfer* mechanism in the classical sense. However, in porous media like soil, heat advection plays a crucial role.
- Convection: Heat is transferred between a surface and a moving fluid. Strictly speaking, convective heat transfer relies on both conduction (diffusion) *and* advection, and thus is not a distinct heat transfer mechanism.

It should be noted that in fluid dynamics, the term convection is used in a broader sense and should not be confused with convective heat transfer. Similar to its definition in heat transfer, convective fluid transport relies on both (mass) diffusion and advection.

The governing equation for transient heat conduction, the so-called heat equation, is derived from Fourier's law of heat conduction and the law of energy conservation. According to Fourier's law, the vector of heat flux density  $\mathbf{q}$ , which is the rate of heat flow per unit area, is proportional to the negative temperature gradient  $\nabla T$  and thermal conductivity  $\lambda$

$$\mathbf{q} = -\lambda \nabla T. \quad (10)$$

The first law of thermodynamics yields

$$\frac{dU}{dt} = \dot{Q} + P \quad (11)$$

with  $U$  denoting the internal energy of a certain volume,  $\dot{Q}$  denoting the heat flux and  $P$  denoting mechanical or electrical power passing the surface  $\Gamma$  of the considered volume  $\Omega$ . Thus, the rate of change of internal energy equals the sum of heat flux and power through the surface. With constant material properties, and using the definition of specific heat capacity  $c = \frac{du}{dT}$  together with  $\frac{dU}{dt} = \rho \int^{\Omega} \frac{du}{dt} dV$ , the rate of change of internal energy can be written as

$$\frac{dU}{dt} = \rho c \int^{\Omega} \frac{\partial T}{\partial t} dV. \quad (12)$$

Further considering that  $\dot{Q} = - \int^{\Gamma} \mathbf{q} \mathbf{n} dA$  and applying the divergence theorem yields

$$\dot{Q} = - \int^{\Omega} \nabla \cdot \mathbf{q} dV. \quad (13)$$

Further considering

$$P = \int^{\Omega} \dot{W} dV \quad (14)$$

with  $\dot{W}$  denoting power density or internal heat generation resulting from mechanical or electrical work, substituting Eqs. (12-14) into Eq. (11) and rearranging yields

$$\int^{\Omega} \left[ \rho c \frac{\partial T}{\partial t} + \nabla \cdot \mathbf{q} - \dot{W} \right] dV = 0. \quad (15)$$

For the volume integral, in order to vanish for an arbitrary volume the integrand must vanish as well, such that

$$\rho c \frac{\partial T}{\partial t} + \nabla \cdot \mathbf{q} = \dot{W} \quad (16)$$

or

$$\rho c \frac{\partial T}{\partial t} - \nabla \cdot \lambda \nabla T = \dot{W}. \quad (17)$$

It should be noticed that in the above derivation, some steps are skipped for conciseness. The complete derivation of the heat equation can be found in any classic textbook on heat transfer. It should also be mentioned, that in general the specific heat capacity and thermal conductivity are temperature-dependent. However, for the temperature ranges relevant for the processes considered in this work, it is safe to assume constant, temperature-independent properties.

Taking advective heat transport into account, the heat equation enhances to

$$\rho c \frac{\partial T}{\partial t} + \rho c \mathbf{q}_D \cdot \nabla T - \nabla \cdot \lambda \nabla T = \dot{W} \quad (18)$$

with  $\mathbf{q}_D$  denoting the vector of Darcy flux. Considering the fact that only the fluid is moved by advection, Eq. (18) for a fully saturated porous medium reads

$$(\rho c)_{eff} \frac{\partial T_s}{\partial t} + (\rho c)_f \mathbf{q}_D \cdot \nabla T_s - \nabla \cdot \lambda_{eff} \nabla T_s = \dot{W}. \quad (19)$$

with effective volumetric heat capacity

$$(\rho c)_{eff} = [\epsilon_s (\rho c)_f + (1 - \epsilon_s) (\rho c)_s] \quad (20)$$

and effective thermal conductivity

$$\lambda_{eff} = [\epsilon_s \lambda_f + (1 - \epsilon_s) \lambda_s]. \quad (21)$$

The indices  $s$  and  $f$  refer to the solid porous matrix and fluid, respectively.

To fully describe a heat transport process, initial (IC) and boundary (BC) conditions are required. The initial state of a system is described by

$$T(x, y, z, t = 0) = T_0(x, y, z). \quad (22)$$

There exist several kinds of boundary conditions, which in general are variable in time:

- Dirichlet or 1<sup>st</sup> kind BC: The value, here temperature  $T$ , is prescribed on a boundary  $\Gamma$ .
- Neumann or 2<sup>nd</sup> kind BC: The derivative, here heat flux  $\mathbf{q}_n = \frac{\partial T}{\partial n} \mathbf{n}$ , is specified on a boundary  $\Gamma$ . The index  $\mathbf{n}$  denotes the normal direction. For example, in heat transfer this BC is applied to insulated boundaries with  $\mathbf{q}_n = 0$ .
- Robin or 3<sup>rd</sup> kind BC: A weighted combination of both Dirichlet and Neumann BCs is imposed on a boundary  $\Gamma$ , such that  $aT + b\frac{\partial T}{\partial n} = c$ . For example, in heat transfer this BC is applied for convection boundaries with  $\alpha(T_{surf} - T_\infty) = -\lambda\frac{\partial T}{\partial n}$ . Here,  $\alpha$  denotes the heat transfer coefficient,  $T_{surf}$  denotes the unknown surface temperature and  $T_\infty$  denotes the known fluid temperature.
- Cauchy or 4<sup>th</sup> kind BC: Dirichlet and Neumann BCs are prescribed simultaneously on a boundary  $\Gamma$ , i.e. both  $T$  and  $\mathbf{q}_n$  have to be satisfied. For example, in heat transfer this BC occurs at contacting interfaces of two solids.

Other BCs, e.g. for radiation, can be derived by applying the energy balance at the corresponding boundary.

### 3.2 GROUNDWATER FLOW

The groundwater flow equation is derived from the law of mass conservation. It is analog to the heat equation (Eq. (16)), which is derived from energy balance, and reads

$$S_s \frac{\partial h}{\partial t} + \nabla \cdot \mathbf{q}_D = G. \quad (23)$$

Here,  $S_s$  denotes the storage coefficient,  $h$  denotes the hydraulic head and  $G$  denotes the production term. The above equation is derived under several assumptions, amongst others the incompressibility of both porous matrix and groundwater and constant atmospheric pressure. As in this work only steady-state groundwater flow without sinks or sources are considered, Eq. (23) can be simplified to

$$\nabla \cdot \mathbf{q}_D = 0. \quad (24)$$

Darcy's law is the constitutive equation for fluid flow in porous media. It is analog to Fourier's law (Eq. (10)) and reads

$$\mathbf{q}_D = -k_f \nabla h \quad (25)$$

with the hydraulic conductivity  $k_f$ , which is a function of gravity, the porous media permeability, and the fluids density and dynamic viscosity. It can be shown that Darcy's law is a solution of the Navier-Stokes equations. In the form presented above, it is only valid for

laminar flow. Additional forms exist for special cases. For a full overview and derivation of groundwater flow and Darcy equations, corresponding textbooks should be consulted.

In practice, boundary conditions of 1<sup>st</sup> and 2<sup>nd</sup> kind are relevant for the solution of the groundwater flow equation.



# 4

---

## NUMERICS

---

In the first section of this chapter, the underlying concept of the BHE model and its governing equations are provided. Next, the finite element discretisation of the BHE equations is demonstrated. The heat pump model developed in this work is presented in the last section of this chapter.

The entire numerical model was implemented in *OpenGeoSys* (OGS), a finite element simulator for coupled thermo-hydraulic-mechanical-chemical (THMC) processes in porous media (cf. Kolditz et al. [44]).

### 4.1 DUAL-CONTINUUM APPROACH

The BHE model used in this work is based on the dual-continuum approach (DCA), which was originally proposed by Al-Khoury et al. [45] and further extended by Diersch et al. [46], [47]. Here, the BHE is idealised as 1D line elements, which are embedded in a 3D mesh (cf. Fig. 4). The line elements sit on the edges of the 3D elements, such that they share the same nodes.

As shown in Fig. 1, a BHE consists of several components like pipes and grout. At the interfaces between these components, including the borehole wall (which is the interface between grout and surrounding subsurface), mathematically speaking Robin or Cauchy boundary conditions would apply. The first one would represent a case where a contact resistance between the contacting materials appears, such that the heat flow equals on both sides while the temperature at the interface is discontinuous due to the thermal resistance. The second boundary condition would represent a case without an interface resistance, such that the equality of both heat flux and temperature would have to be satisfied. In conventional modelling approaches, where the BHE is fully discretised (cf. Boockmeyer and Bauer [48]), the Cauchy boundary condition is automatically satisfied due to the mesh connectivity. In the DCA, the BHE and its components do not have a spatial extent. Instead, the components are lumped onto points, while the heat transfer processes inside the BHE as well as between the BHE and the surrounding soil are modelled by means of an extended thermal capacity-resistor model (TCRM) proposed by Bauer [49]. The TCRM is derived in analogy to electrical cir-

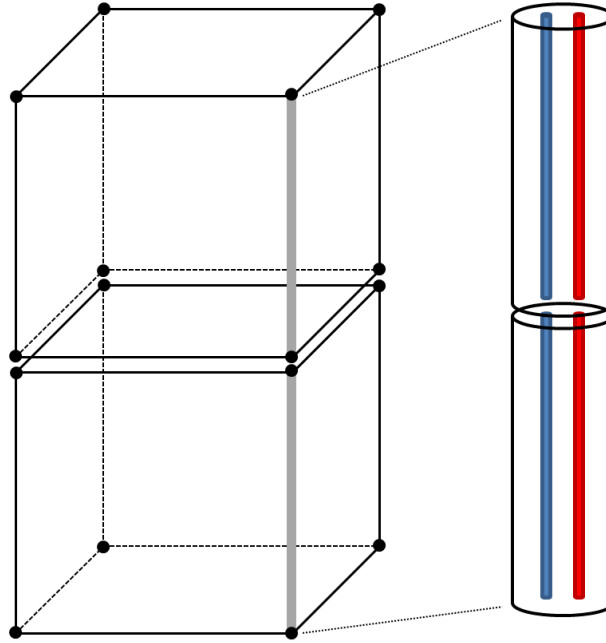


Figure 4: Schematic sketch as exploded view of a mesh for the dual-continuum approach. The subsurface mesh is constructed of 3D elements (here the cubes), while the BHE is lumped onto line elements (bold grey lines). Line elements are sitting on the edges of 3D elements, sharing the same nodes.

cuits. In Fig. 5, such a thermal network is shown for a 1U-type BHE. The degrees of freedom (DOF) assigned to the different BHE components are denoted by temperature  $T$  with indices  $i, o, g, s$  representing the inlet pipe, outlet pipe, grout zones and soil, respectively. The thermal resistances are denoted by  $R$  with the corresponding indices, while the grout's heat capacity is denoted by  $C_g$ . The BHE is coupled to the surrounding subsurface via the soil temperature, thus the soil temperature on the BHE node represents the borehole wall temperature. The governing equations for the BHE are derived from the law of energy conservation. The coupling between the different parts is realised with additional heat exchange terms of the form  $q = \Phi \Delta T$ , which are derived from the actual TCRM, such that the heat flux  $q$  is driven by a temperature difference  $\Delta T$  and the heat transfer coefficient  $\Phi$ . This is necessary as due to lumping, the interfaces are not explicitly represented and such contact boundary conditions are not applicable.

The governing equations and heat exchange terms are now demonstrated for a 1U-type BHE with indices  $i1$  for the inlet pipe,  $o1$  for the outlet pipe,  $g1, g2$  for the two grout zones and  $s$  for soil, respectively the borehole wall (cf. Fig. 5). In the pipes, advection of the heat

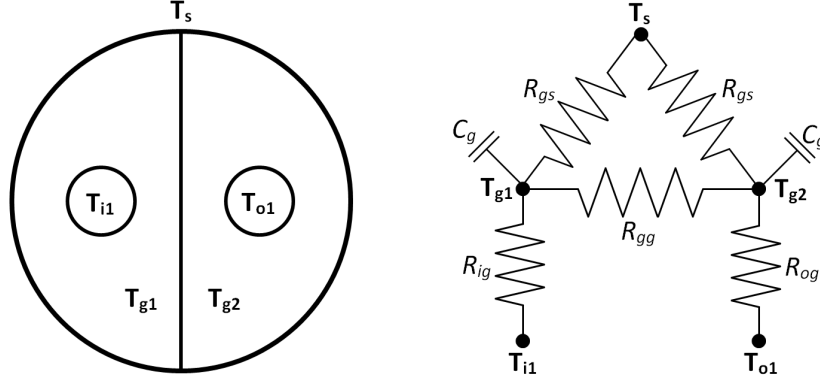


Figure 5: Schematic of a 1U-type BHE for the dual-continuum approach, reproduced after [46]: Degrees of freedom (left), thermal capacity-resistor network (right).

carrier fluid  $h$  with velocity vector  $\mathbf{v}$  is the controlling heat transport mechanism, such that the governing equation reads

$$(\rho c)_h \frac{\partial T_k}{\partial t} + (\rho c)_h \mathbf{v} \cdot \nabla T_k - \nabla \cdot (\lambda_h \nabla T_k) = H_k \quad \text{in } \Omega_k \text{ for } k = i1, o1 \quad (26)$$

with heat exchange terms:

$$\begin{aligned} -\Phi_{ig} (T_{g1} - T_{i1}) &= q_{nT_{i1}} \text{ on } \Gamma_{i1} \text{ and} \\ -\Phi_{og} (T_{g2} - T_{o1}) &= q_{nT_{o1}} \text{ on } \Gamma_{o1}. \end{aligned} \quad (27)$$

Here,  $\Omega_k$  and  $\Gamma_k$  refer to the BHE components and the corresponding boundaries. The thermal conductivity of the heat carrier fluid is denoted by  $\lambda_h$ , while for simplicity thermal dispersivity of the fluid is neglected here.  $H_k$  on the right-hand side denotes the sink or source term, which is absent in common applications. Following the TCRM, here the heat flows only between the pipes and the corresponding grout zones (cf. Fig. 5). For the grout zones  $g1, g2$ , heat transfer is controlled by conduction, such that

$$(1 - \epsilon_g)(\rho c)_g \frac{\partial T_k}{\partial t} - \nabla \cdot [(1 - \epsilon_g)\lambda_g \nabla T_k] = H_k \quad \text{in } \Omega_k \text{ for } k = g1, g2 \quad (28)$$

with heat exchange terms:

$$\begin{aligned} -\Phi_{gs} (T_s - T_{g1}) - \Phi_{ig} (T_{i1} - T_{g1}) - \Phi_{gg} (T_{g2} - T_{g1}) &= q_{nT_{g1}} \\ &\text{on } \Gamma_{g1} \text{ and} \\ -\Phi_{gs} (T_s - T_{g2}) - \Phi_{og} (T_{o1} - T_{g2}) - \Phi_{gg} (T_{g1} - T_{g2}) &= q_{nT_{g2}} \\ &\text{on } \Gamma_{g2}. \end{aligned} \quad (29)$$

From the heat exchange terms it can be seen that all components are involved now (also indicated in Fig. 5). In the equations above, the heat transfer coefficients  $\Phi$  are related to the actual thermal resistances  $R$  and the specific heat exchange surface  $S$  in the form of

$$\Phi = \frac{1}{R} \frac{1}{S}. \quad (30)$$

The thermal resistance values  $R$  for the different BHE components and BHE types again are derived from physical, material and geometric parameters (cf. [49]). Details on the computation of  $\Phi$ ,  $R$  and  $S$  values for 1U, 2U, CXA and CXC types can be found in [46].

#### 4.2 FINITE ELEMENT REALISATION

The governing equations for the heat transport and groundwater flow processes are discretised by means of the Galerkin Finite Element Method (GFEM) (cf. Zienkiewicz et al. [50]). The approach is demonstrated here for the BHE equations using the example of a 1U-type BHE. As the same procedure applies for the governing equations for heat transport in soil and the groundwater flow equation (cf. Kolditz [51]), they will not be further discussed in this work.

First, the weak statements of the local problem, Eqs. (26) & (28), are formulated by introducing the *test functions*  $\omega$ , together with the substituted heat exchange terms (Eqs. (27) & 29)). The integral forms then read

$$\begin{aligned} \int^{\Omega_k} \left[ \omega (\rho c)_h \left( \frac{\partial T_k}{\partial t} + \mathbf{v} \cdot \nabla T_k \right) + \nabla \omega \cdot \left( \lambda_h \nabla T_k \right) \right] d\Omega \\ + \int^{\Gamma_k} \omega q_{nT_k} d\Gamma = 0 \\ \text{for } k = i1, o1 \end{aligned} \quad (31)$$

for the pipes and

$$\begin{aligned} \int^{\Omega_k} \left[ \omega \left( (1 - \epsilon_g) (\rho c)_g \right) \frac{\partial T_k}{\partial t} + \nabla \omega \cdot \left( (1 - \epsilon_g) \lambda_g \nabla T_k \right) \right] d\Omega \\ + \int^{\Gamma_k} \omega q_{nT_k} d\Gamma = 0 \\ \text{for } k = g1, g2 \end{aligned} \quad (32)$$

for the grout zones. Please note that the source term  $H_k$  is dropped in the equations above, as it doesn't play a role in practical applications. In GFEM, the unknown variables (here  $T$ ) are approximated by *trial functions*, which are identical to the *test functions*  $\omega$ . Eqs. (31) & (32) can be written in the matrix form

$$\mathbf{M}^B \cdot \dot{\mathbf{T}}^B - (\mathbf{L}^B + \mathbf{R}^B) \cdot \mathbf{T}^B + \mathbf{R}^{BS} \cdot \mathbf{T}^S = \mathbf{0}. \quad (33)$$

The upper indices  $B$  and  $S$  refer to the BHE and soil part, respectively, while the upper dot denotes the time derivative. The mass matrix  $\mathbf{M}^B$  is filled with submatrices on the diagonal, which read

$$\mathbf{M}_k = \sum^e \int^{\Omega_k^e} [(\rho c)_h N_i N_j] d\Omega^e \text{ for } k = i1, o1 \quad (34)$$

and

$$\mathbf{M}_k = \sum^e \int^{\Omega_k^e} [(\rho c)_g N_i N_j] d\Omega^e \text{ for } k = g1, g2. \quad (35)$$

The trial/test functions  $\omega$  are denoted by  $N_i$  in matrix form. The summation is carried out over the finite elements  $e$ . The Laplace matrix  $\mathbf{L}^B$  has the same structure, with the submatrices

$$\mathbf{L}_k = \sum^e \int^{\Omega_k^e} [N_i (\rho c)_h \nabla N_j + \nabla N_i \cdot (\lambda_h \cdot \nabla N_j)] d\Omega^e \text{ for } k = i1, o1 \quad (36)$$

and

$$\mathbf{L}_k = \sum^e \int^{\Omega_k^e} [\nabla N_i \cdot (\lambda_g \cdot \nabla N_j)] d\Omega^e \text{ for } k = g1, g2. \quad (37)$$

The  $\mathbf{R}$  matrices contain the heat exchange terms in the general form

$$\mathbf{R} = \sum^e \int^{\Gamma_k^e} \Phi N_i N_j d\Gamma^e \text{ for } k = i1, o1, g1, g2 \quad (38)$$

with the index  $B$  referring to the heat exchange terms inside the BHE, i.e. between pipes and grout, and the index  $BS$  referring to the heat exchange terms between the BHE and the surrounding subsurface, i.e. between grout and soil part.

For the entire heat transport process, the equations of the local problem (the BHE model) have to be assembled into a global equation system together with the heat transport equations of the soil part. The global matrix system reads

$$\begin{pmatrix} \mathbf{M}^S & \mathbf{0} \\ \mathbf{0} & \mathbf{M}^B \end{pmatrix} \cdot \begin{pmatrix} \dot{\mathbf{T}}^S \\ \dot{\mathbf{T}}^B \end{pmatrix} - \begin{pmatrix} \mathbf{L}^* & \mathbf{R}^{SB} \\ \mathbf{R}^{BS} & \mathbf{L}^B \end{pmatrix} \cdot \begin{pmatrix} \mathbf{T}^S \\ \mathbf{T}^B \end{pmatrix} = \begin{pmatrix} \mathbf{H}^S \\ \mathbf{0} \end{pmatrix} \quad (39)$$

with  $\mathbf{L}^* = \mathbf{L}^S - \mathbf{R}^B$ ,  $\mathbf{R}^{SB} = \mathbf{R}^{BS}$ , and  $\mathbf{H}^S$  denoting the source/sink term for the soil part. Applying fully implicit Euler time discretisation yields

$$\begin{pmatrix} \mathbf{A}^S & \mathbf{R}^{SB} \\ \mathbf{R}^{BS} & \mathbf{A}^B \end{pmatrix} \cdot \begin{pmatrix} \mathbf{T}^S \\ \mathbf{T}^B \end{pmatrix}_{n+1} = \begin{pmatrix} \mathbf{B}^S \\ \mathbf{B}^B \end{pmatrix}_{n+1,n} \quad (40)$$

with  $n$  and  $n+1$  denoting the previous and current time step. The submatrices read

$$\begin{aligned} \mathbf{A}^S &= \frac{1}{\Delta t_n} \mathbf{M}^S - \mathbf{L}^* \\ \mathbf{B}^S &= \frac{1}{\Delta t_n} \mathbf{M}^S \cdot \mathbf{T}^S_n + \mathbf{W}^S_{n+1} \\ \mathbf{A}^B &= \frac{1}{\Delta t_n} \mathbf{M}^B - \mathbf{L}^B \\ \mathbf{B}^B &= \frac{1}{\Delta t_n} \mathbf{M}^B \cdot \mathbf{T}^B_n \end{aligned} \quad (41)$$

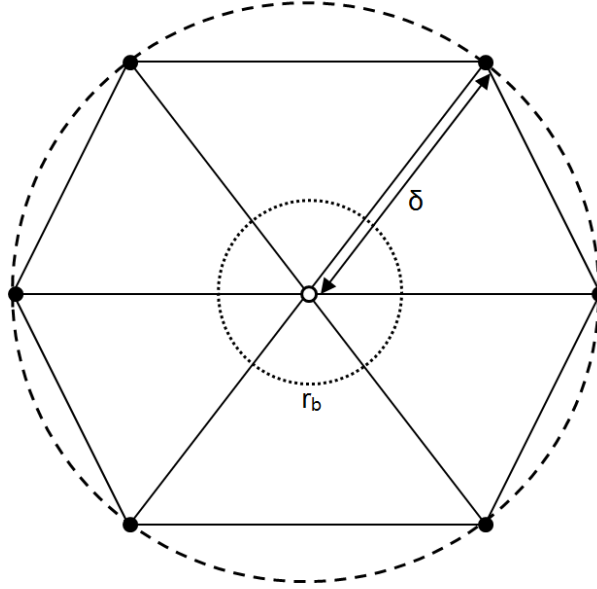


Figure 6: Finite element mesh around the BHE node with  $n = 6$ , reproduced after [47].

with  $\Delta t_n = t_{n+1} - t_n$  denoting the time step size.

It should be noticed, that the heat exchange terms  $\mathbf{R}^{\text{SB}} \cdot \mathbf{T}^{\text{B}}$  and  $\mathbf{R}^{\text{BS}} \cdot \mathbf{T}^{\text{S}}$  are linearly dependent on the soil and BHE temperature DOFs. That means, when the solution changes, the heat fluxes change as well. For this reason, a Picard iteration scheme is employed to achieve a converged solution. Furthermore, the processes are sequentially coupled. First, the groundwater flow process is solved, and the resulting Darcy flux field is passed to the heat transport process, which is solved afterwards. Details on the implementation of the entire numerical model in OGS are provided in Shao et al. [52].

With the DCA, the BHE is reduced to line elements, such that it is represented by a single node in a horizontal section (cf. Fig. 6). As this results in a nodal singularity, the mesh requires special attention to ensure the correct heat flux over the borehole wall. More specifically, the distance between the BHE node and the surrounding nodes determines this heat flux. Diersch et al. [47] proposed a method to estimate the optimal nodal distance  $\delta$  based on the number of surrounding nodes  $n$  and the borehole radius  $r_b$

$$\delta = ar_b, \quad a = e^{\frac{2\pi}{\vartheta}}, \quad \vartheta = n \tan \frac{\pi}{n}. \quad (42)$$

With increasing number of surrounding nodes, the nodal distance increases as well. It is of highest importance to design the mesh according to Eq. (42), as all DOFs of the BHE are controlled by the heat flux over the borehole wall.

## 4.3 HEAT PUMP MODEL

In the BHE model, boundary conditions are always imposed in terms of inlet temperature  $T_{i1}$ . The heat flux through an entire BHE  $\dot{Q}_{BHE}$  can be expressed by the temperature difference between inlet and outlet, such that

$$\dot{Q}_{BHE} = (\rho c)_h Q_h (T_{i1} - T_{o1}), \quad (43)$$

with  $Q_h$  referring to the volumetric flow rate of the heat carrier fluid. To prescribe a thermal load together with the flow rate, an iterative scheme has to be employed. The inlet temperature BC of the current iteration  $n + 1$  then reads

$$T_{i1}^{n+1} = T_{o1}^n + \frac{\dot{Q}_{BHE}}{(\rho c)_h Q_h}, \quad (44)$$

using the outlet temperature from the previous iteration  $n$ . In the actual implementation, Picard iterations are performed until a suitable convergence criterion is satisfied (cf. Ch. 4.2). Considering the heat pump's COP and revisiting Eqs. (2) & (4), the BHE load is determined by

$$\dot{Q}_{BHE}^{heating} = \dot{Q}_{Building}^{heating} - W = \dot{Q}_{Building}^{heating} \left(1 - \frac{1}{COP^{heating}}\right) \quad (45)$$

for heating mode and

$$\dot{Q}_{BHE}^{cooling} = \dot{Q}_{Building}^{cooling} + W = \dot{Q}_{Building}^{cooling} \left(1 + \frac{1}{COP^{cooling}}\right) \quad (46)$$

for cooling mode. It should be noticed that, instead in terms of energy, the equations are written in terms of power now. Finally, the above expressions are substituted into Eq. (44), together with the COP value corresponding to the BHE outlet temperature of the previous iteration  $COP = f(T_{o1}^n)$ .

---

MODEL VALIDATION

---

The OGS implementation of the BHE model was validated with experimental results obtained by Beier et al. [53].

## 5.1 EXPERIMENTAL SETUP

In Beier's experiment, a Thermal Response Test (TRT) was performed under controlled conditions on a single U-tube borehole heat exchanger placed inside a wooden box filled with sand. Inlet and outlet fluid temperatures were monitored together with temperatures at the borehole wall and at different locations in the sand. The length of the wooden box is 18.3 m with a square cross section of 1.8 m per side. An aluminium pipe with a wall thickness of 0.3 cm is acting as the borehole wall. Inside of the aluminium pipe, the BHE is centered with spacers and surrounded by the grouting material. Water is acting as the refrigerant. A second wooden box was built around the actual sandbox. In the space between these two boxes, air at a constant temperature was circulated in order to protect the experiment from influences of the ambient air. Detailed parameters of the configuration can be found in Tab. 1.

Table 1: Parameters of the sandbox experiment, cf. [53]

Parameter	Symbol	Value	Unit
Soil thermal conductivity	$\lambda_s$	2.78	$\text{Wm}^{-1}\text{K}^{-1}$
Soil heat capacity	$(\rho c)_s$	$3.2 \times 10^6$	$\text{Jm}^{-3}\text{K}^{-1}$
Borehole diameter	$D_b$	0.13	m
Pipe diameter	$d_p$	0.027	m
Pipe wall thickness	$b_p$	0.003	m
Pipe distance	$w$	0.053	m
Pipe thermal conductivity	$\lambda_p$	0.39	$\text{Wm}^{-1}\text{K}^{-1}$
Grout thermal conductivity	$\lambda_g$	0.73	$\text{Wm}^{-1}\text{K}^{-1}$
Grout heat capacity	$(\rho c)_g$	$3.8 \times 10^6$	$\text{Jm}^{-3}\text{K}^{-1}$



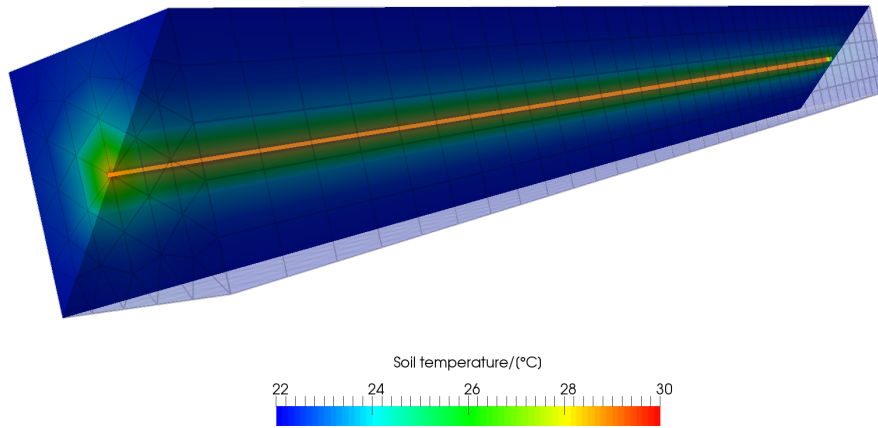


Figure 7: Finite element mesh of the sandbox model, with the BHE indicated by the bold line in the center. The temperature distribution is shown for the final state of the experiment.

## 5.2 MODEL SETUP

The numerical sandbox model is shown in Fig. 7. In the experiment, an aluminium pipe was acting as the borehole wall. As it cannot be represented by the DCA model, the borehole diameter was taken as the aluminium pipe's outer diameter of 0.13 m. The thermal conductivity of the grout was increased from originally  $0.73 \text{ Wm}^{-1}\text{K}^{-1}$  to  $0.806 \text{ Wm}^{-1}\text{K}^{-1}$ , in order to account for the aluminium pipes thermal conductivity and geometry. For the thermal properties and viscosity of the fluid, properties of water are taken at an average temperature of approx.  $36 \text{ }^\circ\text{C}$ .

Initial conditions for fluid inlet/outlet temperatures and wall temperature were directly taken from the measurements at  $t = 0$ . For the initial soil temperature, the mean value of all sensors placed in the sand was taken. For the initial grout temperatures, arithmetic mean values between wall and fluid inlet/outlet temperature were imposed. Detailed initial temperatures can be found in Tab. 2. The boundary conditions on the BHE are prescribed as time series of measured inlet fluid temperature and flow rate, as demonstrated in Fig. 8.

## 5.3 RESULTS

The outlet temperature (Fig. 9), the borehole wall temperature and soil temperatures at 0.24 m and 0.44 m distance to the borehole wall (Fig. 10) were compared to the experimental results. A good match between experimental and simulation results can be observed, with the largest relative error of about 2.5% occurring at the wall temperature. Keeping in mind that the error of temperature, flow rate and

Table 2: Initial conditions of the numerical sandbox model

Parameter	Symbol	Value	Unit
Inlet temperature	$T_{i1}$	22.21	°C
Outlet temperature	$T_{o1}$	21.98	°C
Temperature of first grout zone	$T_{g1}$	22.08	°C
Temperature of second grout zone	$T_{g2}$	21.97	°C
Soil temperature	$T_s$	22.10	°C
Borehole wall temperature	$T_{wall}$	21.95	°C

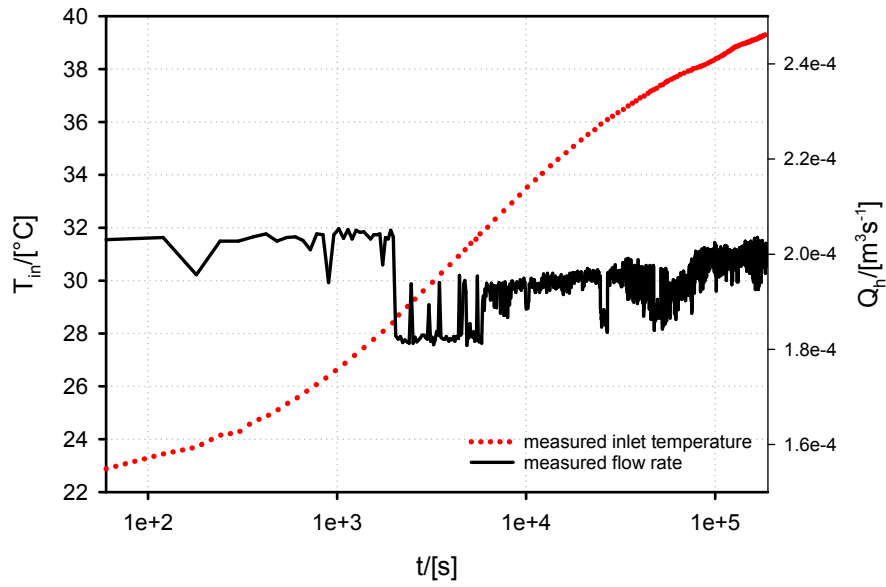


Figure 8: Measured inlet temperature and flow rate of the experiment imposed as boundary conditions in the numerical model, reproduced after Kolditz et al [54].

thermal conductivity measurements are in the same range, the numerical model can be considered to be fully validated.

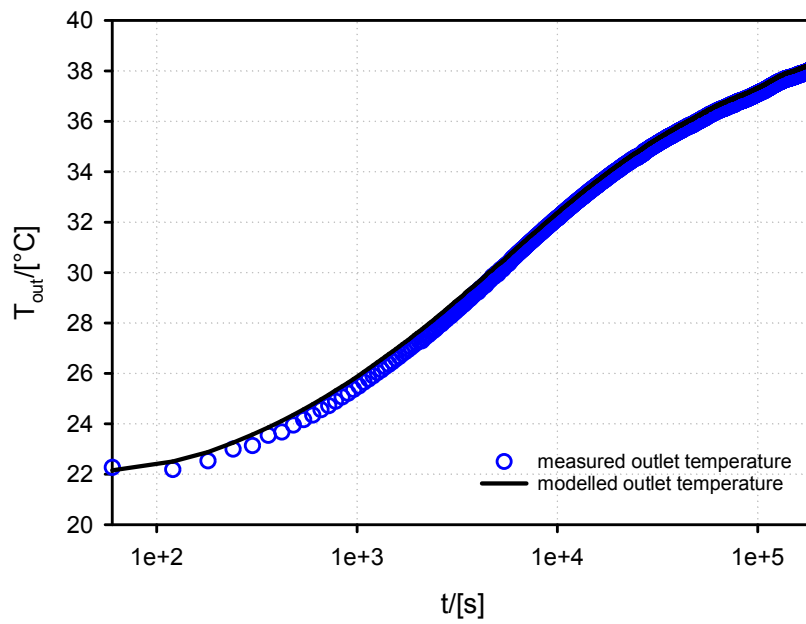


Figure 9: Comparison of measured and simulated outlet temperatures for model validation, reproduced after Kolditz et al [54].

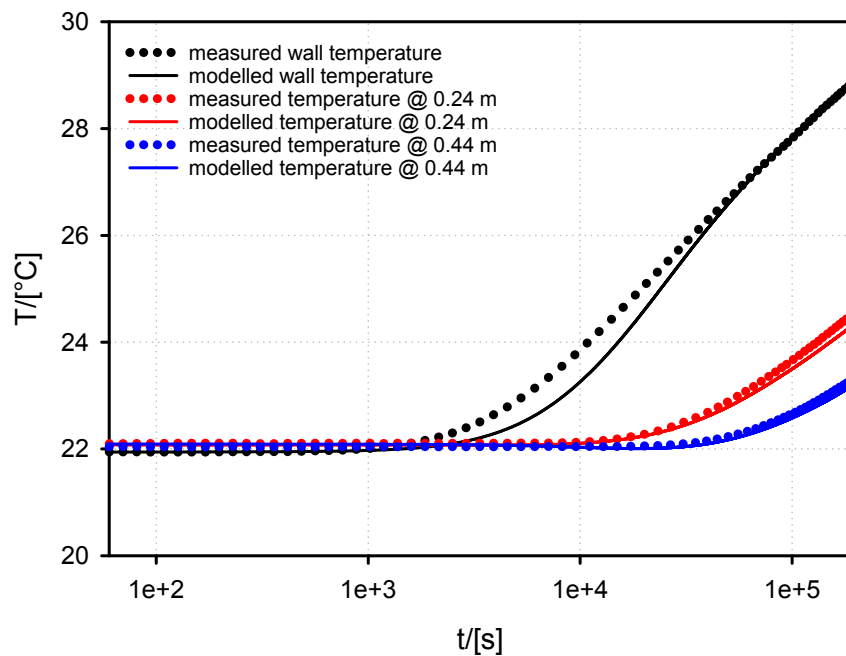


Figure 10: Comparison of measured and simulated temperatures at the borehole wall and in the soil for model validation, reproduced after Kolditz et al [54].

Part II

APPLICATIONS

---

## PREFACE

---

The numerical model presented in Ch. 4 was applied to perform studies on the efficiency and sustainability of BHE-coupled GSHP systems, as well as to aid the quantification of technically extractable shallow geothermal energy. The first two of these studies have been published as peer-reviewed journal papers, while the last one has been submitted. In the following chapters, a short overview of these papers is provided. It is organised such that first the objective of the particular study is delineated. Second, the outcome of the studies is summarised. Last, the references for each paper are given.

---

## SUSTAINABILITY AND EFFICIENCY OF BHE-COUPLED GSHP SYSTEMS

---

### OBJECTIVE

In this study, the impact factors on the sustainability and efficiency of BHE-coupled GSHP system are investigated under consideration of all relevant influencing phenomena. A comprehensive numerical model was constructed to simulate the groundwater flow and heat transport processes in response to the operation of such systems, based on the local parameters of the Leipzig region, Germany. The parameters are varied in a systematic manner to identify the most important factors influencing the efficiency and sustainability and quantify their impact.

### OUTCOME

First, the importance of including the heat pump performance characteristics in the numerical model is demonstrated. Without considering the heat pump, the BHE outlet and soil temperature drop over 30 years will be overestimated by approximately 5 °C and 1.5 °C respectively in the reference model. Computing the energy balance over the first year, it was found that for the reference scenario, only 89 % of the extracted energy is recovered due to natural heat fluxes. The ratio of extracted and recovered energy then approaches 100 % over at least one decade, until the dynamic equilibrium or quasi-steady state is reached. Furthermore, it could be shown that, when properly designed, the subsurface heat capacity and thermal conductivity have only negligible influence on the heat pumps' efficiency. With sufficient groundwater flow, the thermal recovery of the subsurface is considerably facilitated, also leading to an increased COP and thus less consumption of electric energy. The same holds true for additional cooling in summer. However, when active cooling is employed, the financial benefit is decreased, as the heat pump runs also during the summer months (in reverse) at a higher COP in comparison to traditional air-conditioning system. It was also found, that with thermally enhanced grouting materials, i.e. with higher thermal conductivity, the BHE outlet temperatures and thus the efficiency of the

system increases, while barely affecting the subsurface temperature distribution. Last, design and operation errors are investigated. Underestimation of the buildings heating demand and overestimation of the soil's thermal conductivity during the BHE design process lead to a significant performance degradation, in some cases the heat pump even breaks down due to extremely low BHE outflow temperatures. The same holds true when the actual heat pump load excels the design load.

#### REFERENCE

*P. Hein, O. Kolditz, U.-J. Görke, A. Bucher, H. Shao, A numerical study on the sustainability and efficiency of borehole heat exchanger coupled ground source heat pump systems, Applied Thermal Engineering 100 (2016) 421 - 433. doi:10.1016/j.applthermaleng.2016.02.039. (cf. [55], Appendix 1)*

---

## QUANTIFICATION OF TECHNICALLY EXPLOITABLE SHALLOW GEOTHERMAL ENERGY

---

### OBJECTIVE

A common way to estimate the available geothermal potential of the shallow subsurface is to compute the amount of energy  $E$  which can be extracted from a volume  $V$  with volumetric heat capacity  $C$  due to a homogeneous temperature reduction  $\Delta T$

$$E = VC\Delta T. \quad (47)$$

This method is simple and flexible, as it can be mapped onto different stratigraphic units, aquifers, etc. However, the assumption on  $\Delta T$  values which can be achieved by heat extraction technologies like closed-loop (e.g. BHEs) and open-loop systems (wells) from a certain volume are crucial for the estimated amount of extractable energy. The numerical model developed in this work was adopted to simulate the long-term evolution of the subsurface temperature distribution. The concept of *equivalent* uniform temperature drop is introduced to serve as an auxiliary quantity, as in reality the temperature field is non-uniform. Based on the equivalent temperature drop and Eq. (47), a procedure for the estimation of technically exploitable shallow geothermal energy is established.

### OUTCOME

The equivalent temperature drop  $\Delta T_{s,eq}$  is a function of the local setting, like thermal properties and hydrogeological conditions. Furthermore, the system design (i.e. number and arrangement of BHEs, loads, etc.) is determinant for the final results. Along the values of  $\Delta T_{s,eq}$ , which are also dependent on the volume in which it is evaluated, the temperature drop at the boundaries of this volume has to be taken into account as well to draw conclusions about the heat pumps' efficiency. The proposed method for the quantification of the shallow geothermal potential is demonstrated on selected examples. It was found that with the scenarios considered in this study, an equivalent temperature drop in the range of  $-1.8$  °C to  $-4.4$  °C can be achieved. This is equivalent to an amount of annually extractable energy of 3.5



$\text{kWhm}^{-2}\text{a}^{-1}$  to  $8.6 \text{ kWhm}^{-2}\text{a}^{-1}$ . With the proposed procedure, the estimation of geothermal potential is rather conservative, thus allowing for a higher BHE density, respectively the installation of multiple GSHP systems in the vicinity.

#### REFERENCE

*P. Hein, K. Zhu, A. Bucher, O. Kolditz, Z. Pang, H. Shao, Quantification of exploitable shallow geothermal energy by using Borehole Heat Exchanger coupled Ground Source Heat Pump systems, Energy Conversion and Management 127 (2016) 80 - 89. doi:10.1016/j.encoman.2016.08.97. (cf. [56], Appendix 2)*

---

## TECHNICALLY EXPLOITABLE SHALLOW GEOTHERMAL ENERGY: CASE STUDY

---

### OBJECTIVE

Making use of the simplified approach based on Eq. (47), Zhu et al. [6] estimated the geothermal potential of the city of Cologne, Germany, assuming a uniform temperature reduction of 2-6 °C. Thereby, a total amount of extractable energy was computed, with the conclusion that the city's heating demand can be covered for 2.5-25 years by using shallow geothermal energy, but disregarding sustainability aspects in conjunction with exploiting shallow geothermal resources. A similar case study was conducted, based on the parameters of [6] and applying the method for the quantification of technically exploitable geothermal energy proposed in the research paper summarised in Ch. 7. In addition, the economic and environmental impact is investigated.

### OUTCOME

It was found that the estimated city's heating demand can potentially be entirely covered by BHE-coupled GSHP systems similar to the reference system employed in the simulation. The reference system is based on the heating demand of a single-family house. In this case, the equivalent temperature reduction evaluates to -1.6 °C. However, for a more comprehensive estimation, additional scenarios including a more intensive utilisation through BHE arrays, as well as different loading scenarios including cooling should be considered in future studies, together with restrictions due to building density and legal reasons like groundwater protection. The annual operational costs for the reference system average out to approximately 1056 €. The equivalent carbon-dioxide emissions  $CO_{2e}$  depend on the power source for the heat pump. With conventional grid power, the  $CO_{2e}$  emissions reduce to about 45, 57 and 54 % compared to the conventional heating technologies fuel oil, domestic gas and district heating, respectively. With solar electricity, the  $CO_{2e}$  reduction evaluates to approximately 1, 12 and 11 %, accordingly. When the heat pump is powered by the German green electricity mix (which is comprised of wind power,

hydro-electric power, etc.), the  $CO_{2e}$  footprint can be even further reduced.

#### REFERENCE

*P. Hein, K. Zhu, A. Bucher, O. Kolditz, H. Shao, Technically exploitable geothermal energy by using Borehole Heat Exchangers: A revisit of the Cologne case, submitted to Geothermal Energy (cf. [57], Appendix 3)*

Part III

SUMMARY

---

## ACHIEVEMENTS

---

Within this work, the following contributions have been made to the understanding of BHE-coupled GSHP systems:

- The numerical BHE model, based on the dual-continuum approach and implemented in the OpenGeoSys code, has been successfully validated against experimental data.
- A numerical heat pump model, which accounts for the dynamic regulation of the BHE load subject to heat pump load, heat pump performance characteristics and BHE outflow temperatures, was implemented in OGS and coupled to the BHE model. This allows for the realistic simulation of practical applications. Furthermore, with this model the heat pumps' SCOP, electricity consumption and consequently operational costs and equivalent  $CO_2$  emissions can be estimated.
- With the above mentioned features, a comprehensive numerical model including all relevant phenomena was constructed. This includes different BHE designs, heat pump characteristics, groundwater flow, stratigraphic layers with varying physical properties, ground surface temperature fluctuation, geothermal gradient and geothermal heat flux.
- With this model, the most important factors influencing the efficiency and sustainability of BHE-coupled GSHP systems could be identified and quantified. Regarding the site, these are the local thermal regime in the subsurface and at the ground surface, as well as groundwater flow. Regarding the technical system, these are the BHE length, the operational mode and the grouting material. A correct BHE design with precise assumptions on the soil thermal conductivity as well as the load is crucial for the efficiency and sustainability of such systems.
- Simulation results showed that BHE designs following the current valid guidelines in Germany and thus based on analytical solutions, in some cases can lead to significant over- and under dimensioning. This leads to increased investment costs in the first case. In the latter case, the efficiency can be significantly

decreased while operational costs increase. In the worst case, the system breaks down.

- The concept of equivalent temperature drop was introduced. By using this approach, a workflow for the quantification of technically exploitable shallow geothermal energy was established, which is demonstrated by means of a case study.

---

## CONCLUSIONS AND OUTLOOK

---

Within this work, a coupled numerical model for flow and heat transport processes in the subsurface and borehole heat exchangers was utilised and enhanced with a heat pump model. A suitable modelling strategy was developed in order to integrate the phenomena relevant to such systems. The model was applied to perform a numerical study on the efficiency and sustainability of BHE-coupled ground source heat pumps. Furthermore, based on the numerical model a method for the estimation of the shallow geothermal potential was developed and applied to a case study. It could successfully be demonstrated that numerical modelling provides a powerful tool to enhance process understanding, to aid the planning and design process as well as to support approval activities, decision-making processes and energy policy on local and regional scales. With respect to the design of BHE systems, the OGS implementation can be coupled to the optimisation toolbox PEST [58].

As arrays with a large number of BHEs play an important role in the utilisation of shallow geothermal energy, the numerical model should be further enhanced. At the time of submission of this thesis, a corresponding feature in the OGS code is under development, capable of simulating an arbitrary number of BHEs, interconnections and heat pumps. Other on-going research topics encompass the mechanical processes in response to freezing-thawing-cycles in and around BHEs as well as the impact of BHE operation, respectively the perturbation of the subsurface temperature field, on contaminants and microbiology in the soil.

Recent results and their implication regarding the sustainability, efficiency and safety of BHE-coupled GSHP systems should be integrated into existing design guidelines. This holds particularly true for the influence of groundwater flow as well as the consideration of the heat pumps' COP. The thermal interactions occurring in BHE arrays as well as in the presence of high system density and their implications on the efficiency and sustainability need further investigation as well. The findings have to be included into design guidelines, too. Also, suitable methods for the management of shallow thermal resources and approval activities should be developed, regulating the installation of such systems in order to avoid concurrent utilisation and over-exploitation of the subsurface.

---

## LIST OF FIGURES

---

Figure 1	Schematic illustration of different BHE types in the heating mode.	6
Figure 2	Schematic illustration of a 1U BHE in heating mode.	7
Figure 3	Schematic working principle of a heat pump.	10
Figure 4	Schematic sketch of a mesh for the dual-continuum approach.	22
Figure 5	Schematic of a 1U-type BHE for the dual-continuum approach, reproduced after [46].	23
Figure 6	Finite element mesh around the BHE node with $n = 6$ , reproduced after [47].	26
Figure 7	Finite element mesh of the sandbox model.	29
Figure 8	Boundary conditions of the validation model.	30
Figure 9	Result comparison of the model validation, outlet temperature.	31
Figure 10	Result comparison of the model validation, wall and soil temperatures.	31



---

## LIST OF TABLES

---

Table 1	Parameters of the sandbox experiment, cf. [53]	28
Table 2	Initial conditions of the validation model	30

---

## BIBLIOGRAPHY

---

- [1] S. Hähnlein, P. Blum, and P. Bayer. "Shallow geothermal energy - current legal situation". In: *Grundwasser* 16.2 (2011), pp. 69–75. ISSN: 1432-1165. DOI: 10.1007/s00767-011-0162-0.
- [2] S. Bassetti, E. Rohner, S. Signorelli, B. Matthey. *Documentation of damage cases with borehole heat exchangers, final report (Dokumentation von Schadensfällen bei Erdwärmesonden, Schlussbericht)*. URL: <http://www.bfe.admin.ch/php/modules/enet/streamfile.php?file=000000009159.pdf%5C&name=000000260072.pdf> (visited on 08/03/2016).
- [3] J. Sager. "Fehlfunktionsanalyse eines Geothermie-Wärmepumpensystems, Wenn die Rechnung nicht aufgeht". In: *Geothermische Energie* 83 (2016), pp. 16–17. ISSN: 0948-6615.
- [4] I. Stober, K. Bucher. *Geothermie*. Springer Spektrum. Springer-Verlag GmbH Berlin Heidelberg, 2014. ISBN: 978-3-642-41763-4. DOI: {10.1007/978-3-642-41763-4}.
- [5] J. A. Rivera, P. Blum, and P. Bayer. "Analytical simulation of groundwater flow and land surface effects on thermal plumes of borehole heat exchangers". In: *Applied Energy* 146 (2015), pp. 421–433. ISSN: 0306-2619. DOI: 10.1016/j.apenergy.2015.02.035.
- [6] K. Zhu, P. Blum, G. Ferguson, K.-D. Balke, and P. Bayer. "The geothermal potential of urban heat islands". In: *Environmental Research Letters* 5.4 (2010), p. 044002.
- [7] The Association of German Engineers (Verein Deutscher Ingenieure). *VDI guideline 4640: Thermal use of the underground Part 1: Fundamentals, approvals, environmental aspects (VDI Richtlinie 4640: Thermische Nutzung des Untergrunds - Blatt 1: Grundlagen, Genehmigungen, Umweltaspekte*. Berlin, Germany, 2010.
- [8] The Association of German Engineers (Verein Deutscher Ingenieure). *VDI guideline 4640: Thermal use of the underground Part 2: Ground source heat pump systems, draft (VDI Richtlinie 4640: Thermische Nutzung des Untergrunds - Blatt 2: Erdgekoppelte Wärmepumpenanlagen, Entwurf)*. Berlin, Germany, 2015.
- [9] P. Atkins, J. de Paula. *Atkins' Physical Chemistry*. Oxford University Press, 2014. ISBN: 978-0199697403.
- [10] F. Stauffer, P. Bayer, P. Blum, N. Molina-Giraldo, W. Kinzelbach. *Thermal Use of Shallow Groundwater*. CRC Press. Taylor & Francis Group, LLC, 2014. ISBN: 978-1-4665-6019-2.

- [11] N. Molina-Giraldo, P. Blum, K. Zhu, P. Bayer, and Z. Fang. "A moving finite line source model to simulate borehole heat exchangers with groundwater advection". In: *International Journal of Thermal Sciences* 50.12 (2011), pp. 2506–2513. ISSN: 1290-0729. DOI: 10.1016/j.ijthermalsci.2011.06.012.
- [12] P. Eskilson. "Thermal analysis of heat extraction boreholes". PhD thesis. Lund University, 1987. ISBN: 91-7900-298-6.
- [13] M. Li and A. C. Lai. "Review of analytical models for heat transfer by vertical ground heat exchangers (GHEs): A perspective of time and space scales". In: *Applied Energy* 151 (2015), pp. 178–191. ISSN: 0306-2619. DOI: 10.1016/j.apenergy.2015.04.070.
- [14] R. A. Beier. "Transient heat transfer in a U-tube borehole heat exchanger". In: *Applied Thermal Engineering* 62.1 (2014), pp. 256–266. ISSN: 1359-4311. DOI: 10.1016/j.applthermaleng.2013.09.014.
- [15] J. Claesson, S. Javed. "An Analytical Method to Calculate Borehole Fluid Temperatures for Time-scales from Minutes to Decades". In: *ASHRAE Transactions* 117.2 (2011).
- [16] A. Angelotti, L. Alberti, I. L. Licata, and M. Antelmi. "Energy performance and thermal impact of a Borehole Heat Exchanger in a sandy aquifer: Influence of the groundwater velocity". In: *Energy Conversion and Management* 77 (2014), pp. 700–708. ISSN: 0196-8904. DOI: 10.1016/j.enconman.2013.10.018.
- [17] J. Luo, J. Rohn, M. Bayer, A. Priess, and W. Xiang. "Analysis on performance of borehole heat exchanger in a layered subsurface". In: *Applied Energy* 123 (2014), pp. 55–65. ISSN: 0306-2619. DOI: 10.1016/j.apenergy.2014.02.044.
- [18] R. Perego, R. Guandalini, L. Fumagalli, F. Aghib, L. D. Biase, and T. Bonomi. "Sustainability evaluation of a medium scale GSHP system in a layered alluvial setting using 3D modeling suite". In: *Geothermics* 59, Part A (2016), pp. 14–26. ISSN: 0375-6505. DOI: 10.1016/j.geothermics.2015.10.003.
- [19] T. V. Bandos, A. Montero, E. Fernandez, J. L. G. Santander, J. M. Isidro, J. Perez, P. J. F. de Cordoba, and J. F. Urchueguia. "Finite line-source model for borehole heat exchangers: effect of vertical temperature variations". In: *Geothermics* 38.2 (2009), pp. 263–270. ISSN: 0375-6505. DOI: 10.1016/j.geothermics.2009.01.003.
- [20] T. Kurevija, D. Vulin, V. Krapec. "Influence of Undisturbed Ground Temperature and Geothermal Gradient on the Sizing of Borehole Heat Exchangers". In: *World Renewable Energy Congress 2011* (2011), pp. 1360–1367.

- [21] A. Bidarmaghz, G. A. Narsilio, I. W. Johnston, and S. Colls. "The importance of surface air temperature fluctuations on long-term performance of vertical ground heat exchangers". In: *Geomechanics for Energy and the Environment* 6 (2016). Themed Issue on Selected Papers Symposium of Energy Geotechnics 2015 Part I, pp. 35–44. ISSN: 2352-3808. DOI: 10.1016/j.gete.2016.02.003.
- [22] M. Bortoloni, M. Bottarelli, and Y. Su. "A study on the effect of ground surface boundary conditions in modelling shallow ground heat exchangers". In: *Applied Thermal Engineering* (2016). ISSN: 1359-4311. DOI: 10.1016/j.applthermaleng.2016.05.063.
- [23] M. de Paly, J. Hecht-Mendez, M. Beck, P. Blum, A. Zell, and P. Bayer. "Optimization of energy extraction for closed shallow geothermal systems using linear programming". In: *Geothermics* 43 (2012), pp. 57–65. ISSN: 0375-6505. DOI: 10.1016/j.geothermics.2012.03.001.
- [24] M. Beck, P. Bayer, M. de Paly, J. Hecht-Mendez, and A. Zell. "Geometric arrangement and operation mode adjustment in low-enthalpy geothermal borehole fields for heating". In: *Energy* 49 (2013), pp. 434–443. ISSN: 0360-5442. DOI: 10.1016/j.energy.2012.10.060.
- [25] M. Yu, K. Zhang, X. Cao, A. Hu, P. Cui, and Z. Fang. "Zoning operation of multiple borehole ground heat exchangers to alleviate the ground thermal accumulation caused by unbalanced seasonal loads". In: *Energy and Buildings* 110 (2016), pp. 345–352. ISSN: 0378-7788. DOI: 10.1016/j.enbuild.2015.11.022.
- [26] W. Retkowski, G. Ziefle, and J. Thöming. "Evaluation of different heat extraction strategies for shallow vertical ground-source heat pump systems". In: *Applied Energy* 149 (2015), pp. 259–271. ISSN: 0306-2619. DOI: 10.1016/j.apenergy.2015.03.004.
- [27] S. Koochi-Fayegh and M. Rosen. "An analytical approach to evaluating the effect of thermal interaction of geothermal heat exchangers on ground heat pump efficiency". In: *Energy Conversion and Management* 78 (2014), pp. 184–192. ISSN: 0196-8904. DOI: 10.1016/j.enconman.2013.09.064.
- [28] T. Kurevija, D. Vulin, and V. Krapec. "Effect of borehole array geometry and thermal interferences on geothermal heat pump system". In: *Energy Conversion and Management* 60 (2012). Special issue of Energy Conversion and Management dedicated to {ECOS} 2011 - the 24th International Conference on Efficiency, Costs, Optimization, Simulation and Environmental Impact of Energy Systems, pp. 134–142. ISSN: 0196-8904. DOI: 10.1016/j.enconman.2012.02.012.

- [29] A. Gultekin, M. Aydin, and A. Sisman. "Thermal performance analysis of multiple borehole heat exchangers". In: *Energy Conversion and Management* 122 (2016), pp. 544–551. ISSN: 0196-8904. DOI: 10.1016/j.enconman.2016.05.086.
- [30] M. D. Rosa, F. Ruiz-Calvo, J. M. Corberan, C. Montagud, and L. A. Tagliafico. "A novel TRNSYS type for short-term borehole heat exchanger simulation: B2G model". In: *Energy Conversion and Management* 100 (2015), pp. 347–357. ISSN: 0196-8904. DOI: 10.1016/j.enconman.2015.05.021.
- [31] L. Dai, Y. Shang, X. Li, and S. Li. "Analysis on the transient heat transfer process inside and outside the borehole for a vertical U-tube ground heat exchanger under short-term heat storage". In: *Renewable Energy* 87, Part 3 (2016). Sustainable energy utilization in cold climate zone (Part II), pp. 1121–1129. ISSN: 0960-1481. DOI: 10.1016/j.renene.2015.08.034.
- [32] S. Erol, M. A. Hashemi, and B. Francois. "Analytical solution of discontinuous heat extraction for sustainability and recovery aspects of borehole heat exchangers". In: *International Journal of Thermal Sciences* 88 (2015), pp. 47–58. ISSN: 1290-0729. DOI: 10.1016/j.ijthermalsci.2014.09.007.
- [33] T. Sliwa, M. A. Rosen. "Natural and Artificial Methods for Regeneration of Heat Resources for Borehole Heat Exchangers to Enhance the Sustainability of Underground Thermal Storages: A Review". In: *Sustainability* 7 (2015), pp. 13104–13125. ISSN: 2071-1050. DOI: 10.3390/su71013104.
- [34] P. Mielke, D. Bauer, S. Homuth, A. E. Götz, I. Sass. "Thermal effect of a borehole thermal energy store on the subsurface". In: *Geothermal Energy* 2 (2014), p. 5. ISSN: 2195-9706. DOI: 10.1186/s40517-014-0005-1.
- [35] J. Desmedt, J. Van Bael, H. Hoes, and N. Robeyn. "Experimental performance of borehole heat exchangers and grouting materials for ground source heat pumps". In: *International Journal of Energy Research* 36.13 (2012), pp. 1238–1246. ISSN: 1099-114X. DOI: 10.1002/er.1898.
- [36] C. J. Wood, H. Liu, and S. B. Riffat. "Comparative performance of U-tube and coaxial loop designs for use with a ground source heat pump". In: *Applied Thermal Engineering* 37 (2012), pp. 190–195. ISSN: 1359-4311. DOI: 10.1016/j.applthermaleng.2011.11.015.
- [37] C. Lee, M. Park, S. Min, S.-H. Kang, B. Sohn, and H. Choi. "Comparison of effective thermal conductivity in closed-loop vertical ground heat exchangers". In: *Applied Thermal Engineering* 31.1718 (2011). {SET} 2010 Special Issue, pp. 3669–3676.

- ISSN: 1359-4311. DOI: 10.1016/j.applthermaleng.2011.01.016.
- [38] A. Casasso and R. Sethi. "Efficiency of closed loop geothermal heat pumps: A sensitivity analysis". In: *Renewable Energy* 62 (2014), pp. 737–746. ISSN: 0960-1481. DOI: 10.1016/j.renene.2013.08.019.
- [39] J. Epting, F. Händel, and P. Huggenberger. "Thermal management of an unconsolidated shallow urban groundwater body". In: *Hydrology and Earth System Sciences* 17.5 (2013), pp. 1851–1869. DOI: 10.5194/hess-17-1851-2013.
- [40] P. Blum, G. Campillo, and T. Kölbl. "Techno-economic and spatial analysis of vertical ground source heat pump systems in Germany". In: *Energy* 36.5 (2011), pp. 3002–3011. ISSN: 0360-5442. DOI: 10.1016/j.energy.2011.02.044.
- [41] T. Arola and K. Korkka-Niemi. "The effect of urban heat islands on geothermal potential: examples from Quaternary aquifers in Finland". In: *Hydrogeology Journal* 22.8 (2014), pp. 1953–1967. ISSN: 1435-0157. DOI: 10.1007/s10040-014-1174-5.
- [42] T. Arola, L. Eskola, J. Hellen, and K. Korkka-Niemi. "Mapping the low enthalpy geothermal potential of shallow Quaternary aquifers in Finland". In: *Geothermal Energy* 2.1 (2014), pp. 1–20. ISSN: 2195-9706. DOI: 10.1186/s40517-014-0009-x.
- [43] Y. Zhang, K. Soga, and R. Choudhary. "Shallow geothermal energy application with GSHPs at city scale: study on the City of Westminster". In: *Geotechnique Letters* 4.2 (2014), pp. 125–131. DOI: 10.1680/geolett.13.00061. URL: 10.1680/geolett.13.00061.
- [44] O. Kolditz et al. "OpenGeoSys: an open-source initiative for numerical simulation of thermo-hydro-mechanical/chemical (THM/C) processes in porous media". In: *Environmental Earth Sciences* 67.2 (2012), pp. 589–599. ISSN: 1866-6299. DOI: 10.1007/s12665-012-1546-x.
- [45] R. Al-Khoury, T. Kölbl, and R. Schramedei. "Efficient numerical modeling of borehole heat exchangers". In: *Computers & Geosciences* 36.10 (2010), pp. 1301–1315. ISSN: 0098-3004. DOI: 10.1016/j.cageo.2009.12.010.
- [46] H.-J. Diersch, D. Bauer, W. Heidemann, W. Rühaak, and P. Schätzl. "Finite element modeling of borehole heat exchanger systems: Part 1. Fundamentals". In: *Computers & Geosciences* 37.8 (2011), pp. 1122–1135. ISSN: 0098-3004. DOI: 10.1016/j.cageo.2010.08.003.

- [47] H.-J. Diersch, D. Bauer, W. Heidemann, W. Rühaak, and P. Schätzl. “Finite element modeling of borehole heat exchanger systems: Part 2. Numerical simulation”. In: *Computers & Geosciences* 37.8 (2011), pp. 1136–1147. ISSN: 0098-3004. DOI: 10.1016/j.cageo.2010.08.002.
- [48] A. Boockmeyer and S. Bauer. “High-temperature heat storage in geological media: high-resolution simulation of near-borehole processes”. In: *Gotechnique Letters* 4.2 (2014), pp. 151–156. DOI: 10.1680/geolett.13.00060.
- [49] D. Bauer. “Thermal modelling of borehole heat exchangers and borehole thermal energy stores”. PhD thesis. Institute of Thermodynamics and Thermal Engineering, University of Stuttgart, 2011. DOI: 10.18419/opus-1979.
- [50] O. C. Zienkiewicz, R. L. Taylor, J. Z. Zhu. *The Finite Element Method: Its Basis and Fundamentals*. Elsevier Ltd, Oxford, 2013. ISBN: 978-1856176330.
- [51] O. Kolditz. *Computational Methods in Environmental Fluid Mechanics*. Springer-Verlag Berlin Heidelberg, 2002. ISBN: 978-3-540-42895-4. DOI: {10.1007/978-3-662-04761-3}.
- [52] H. Shao, P. Hein, A. Sachse, O. Kolditz. *Geoenergy Modeling II, Shallow Geothermal Systems*. Computational Modeling of Energy Systems. Springer International Publishing, 2016. ISBN: 978-3-319-45057-5. DOI: {10.1007/978-3-319-45057-5}.
- [53] R. A. Beier, M. D. Smith, and J. D. Spitler. “Reference data sets for vertical borehole ground heat exchanger models and thermal response test analysis”. In: *Geothermics* 40.1 (2011), pp. 79–85. ISSN: 0375-6505. DOI: 10.1016/j.geothermics.2010.12.007.
- [54] O. Kolditz, U.-J. Görke, H. Shao, W. Wang, S. Bauer, ed. *Thermo-Hydro-Mechanical-Chemical Processes in Fractured Porous Media: Modelling and Benchmarking*. Terrestrial Environmental Sciences. Springer International Publishing, 2016. ISBN: 978-3-319-29223-6. DOI: {10.1007/978-3-319-29224-3}.
- [55] P. Hein, O. Kolditz, U.-J. Görke, A. Bucher, and H. Shao. “A numerical study on the sustainability and efficiency of borehole heat exchanger coupled ground source heat pump systems”. In: *Applied Thermal Engineering* 100 (2016), pp. 421–433. ISSN: 1359-4311. DOI: <http://dx.doi.org/10.1016/j.applthermaleng.2016.02.039>.
- [56] P. Hein, K. Zhu, A. Bucher, O. Kolditz, Z. Pang, and H. Shao. “Quantification of exploitable shallow geothermal energy by using Borehole Heat Exchanger coupled Ground Source Heat Pump systems”. In: *Energy Conversion and Management* 127 (2016),

pp. 80–89. ISSN: 0196-8904. DOI: <http://dx.doi.org/10.1016/j.enconman.2016.08.097>.

- [57] P. Hein, K. Zhu, A. Bucher, O. Kolditz, and H. Shao. “Technically exploitable geothermal energy by using Borehole Heat Exchangers: A revisit of the Cologne case”. In: *submitted to Geothermal Energy* (2016).
- [58] PEST. URL: <http://www.pesthomepage.org/> (visited on 08/03/2016).



---

## APPENDIX

---

### 1 PAPER 1

*P. Hein, O. Kolditz, U.-J. Görke, A. Bucher, H. Shao, A numerical study on the sustainability and efficiency of borehole heat exchanger coupled ground source heat pump systems, Applied Thermal Engineering 100 (2016) 421 - 433. doi:10.1016/j.applthermaleng.2016.02.039.*

### 2 PAPER 2

*P. Hein, K. Zhu, A. Bucher, O. Kolditz, Z. Pang, H. Shao, Quantification of exploitable shallow geothermal energy by using Borehole Heat Exchanger coupled Ground Source Heat Pump systems, Energy Conversion and Management 127 (2016) 80 - 89. doi:10.1016/j.encoman.2016.08.97.*

### 3 PAPER 3

*P. Hein, K. Zhu, A. Bucher, O. Kolditz, H. Shao, Technically exploitable geothermal energy by using Borehole Heat Exchangers: A revisit of the Cologne case, submitted to Geothermal Energy*